

Papers published in *Hydrology and Earth System Sciences Discussions* are under open-access review for the journal *Hydrology and Earth System Sciences*

# Reconstructing 20th century global hydrography: a contribution to the Global Terrestrial Network- Hydrology (GTN-H)

D. Wisser<sup>1</sup>, B. M. Fekete<sup>2</sup>, C. J. Vörösmarty<sup>2</sup>, and A. H. Schumann<sup>3</sup>

<sup>1</sup>Institute for the Study of Earth, Oceans, and Space, University of New Hampshire, Durham, New Hampshire, USA

<sup>2</sup>Civil Engineering Department, City College of New York, CUNY, New York, New York, USA

<sup>3</sup>Institute of Hydrology, Water Resources Management and Environmental Engineering, Ruhr-Universität Bochum, Bochum, Germany

Received: 17 March 2009 – Accepted: 20 March 2009 – Published: 26 March 2009

Correspondence to: D. Wisser (dominik.wisser@unh.edu)

Published by Copernicus Publications on behalf of the European Geosciences Union.

**HESSD**

6, 2679–2732, 2009

## Reconstructing 20th century global hydrography

D. Wisser et al.

Title Page

Abstract

Introduction

Conclusions

References

Tables

Figures

◀

▶

◀

▶

Back

Close

Full Screen / Esc

Printer-friendly Version

Interactive Discussion



## Abstract

This paper presents a new reconstruction of the 20th Century global hydrography using fully coupled water balance and transport model in a flexible modeling framework. The modeling framework allows a high level of configurability both in terms of input forcings and model structure. Spatial and temporal trends in hydrological cycle components are assessed under “pre-industrial” conditions (without modern-day human activities) and contemporary conditions (incorporating the effects of irrigation and reservoir operations). The two sets of simulations allow the isolation of the trends arising from variations in the climate input driver alone and from human interventions. Our findings confirm that the expansion of irrigation and the construction has significantly and gradually impacted hydrological components in individual river basins. Variations in the volume of water entering the oceans, however, are governed by variations in the climate signal alone with human activities playing secondary role. Globally, we do find a significant trend in the terrestrial discharge over the last century.

The largest impact of human intervention on the hydrological cycle arises from the operation of reservoirs that drastically changes the seasonal pattern of horizontal water transport in the river system and thereby directly and indirectly affects a number of processes.

## 1 Introduction

Humans have greatly altered the hydrological cycle over the last century. Global water withdrawal has increased by 700% during the last century (Ghassemi and White, 2007) and is expected to further rise as the world’s population continues growing. Such alterations affect the magnitude and the timing of runoff and river flow, and has been amply documented. These impacts include abstraction of water for irrigation and the distortions of discharge imposed by reservoirs alter the temporal pattern of river discharge (Bouwer et al., 2006; Haddeland et al., 2006a; Shibuo et al., 2007), the impacts of in-

HESSD

6, 2679–2732, 2009

## Reconstructing 20th century global hydrography

D. Wisser et al.

Title Page

Abstract

Introduction

Conclusions

References

Tables

Figures

◀

▶

◀

▶

Back

Close

Full Screen / Esc

Printer-friendly Version

Interactive Discussion



## Reconstructing 20th century global hydrography

D. Wisser et al.

Title Page

Abstract

Introduction

Conclusions

References

Tables

Figures

◀

▶

◀

▶

Back

Close

Full Screen / Esc

Printer-friendly Version

Interactive Discussion



creased evapotranspiration due to land cover changes that could potentially affect local climate (Douglas et al., 2006; Kueppers et al., 2007), and construction of large reservoirs that have tripled the mean age of water at the mouth of river basins (Vörösmarty et al., 1997). Furthermore, changes in observed streamflow over the last century and model simulations show coherent trends (increases in eastern Africa and high-latitude regions and decreases in southern Africa, southern Europe and the middle East) in the availability of freshwater predicted in a changing climate (Milly et al., 2005).

The abstraction of water for irrigation purposes lowers the volume of water entering rivers but has also been shown to impact the seasonality of river flow by increasing, for example in the temperate zone, winter river discharge should water returning from irrigated areas become runoff (Kendy and Bredehoeft, 2006). Such alterations in the hydrological cycle do not only impact the spatial and temporal distribution of runoff but have direct and indirect effects on the bio-geophysical state of water resources and thereby on the sustainability of water resources.

The changes in the apparent aging of water on river systems as a result of reservoir impoundments, greatly affect the re-aeration capacity of the river, which in turn, determines the ability of the water to decompose organic matter. Reservoirs impact the sediment retention of major river (Vörösmarty et al., 2003), the emission of trace gas emissions (Soumis et al., 2004; Galy-Lacaux et al., 1999; St. Louis et al., 2000) and the cycling of nutrients (Seitzinger et al., 2002). The global water cycle is therefore not affected by the changes in the weather and climate system alone but also by additional sources of human interventions (Vörösmarty, 2002), the most notable of which at the scale this study is concerned with are increased evapotranspiration due to expansion of irrigated areas and the distortion of streamflow by large impoundments (Vörösmarty and Sahagian, 2000).

The purpose of this paper is to analyze trends in components of the global hydrological cycle over in the 20th century and to investigate the contribution of human interventions to changes in those components. We use a water balance modeling approach that explicitly accounts for such interventions when forced by time series of observed

climate data.

After a brief description of the model and data we present a validation of the model predictions against a large set of discharge data and discuss the development of water abstractions over the last century. Time series of modeled discharge (under natural and disturbed conditions) entering the oceans and internally draining basins are discussed. We illustrate the impacts of time varying irrigated areas and reservoirs for a set of representative river basins.

## 2 Methods

### 2.1 The WBM<sub>plus</sub> model

To simulate components of the hydrological cycle, we used WBM<sub>plus</sub>, an extension of a grid based water balance and transport algorithm (Federer et al., 2003; Rawlins et al., 2003; Vörösmarty et al., 1998). WBM<sub>plus</sub> is a fully coupled water balance and transport model that simulates the vertical water exchange between the land surface and the atmosphere and the horizontal water transport along prescribed river network. It is implemented in the recently developed modeling Framework for Aquatic Modeling in the Earth System (FrAMES, Wollheim et al., 2008), which was designed to enable applications of coupled hydrological/biogeochemical models at scales ranging from local (grid cell size in the range of a few hundred meters) to continental and global (grid cell size ranging from 6 min to 30 min), operating at a daily time step. Modeling frameworks have been designed to increase the inter-operability and portability of software among developers, and to increase the efficiency of software development through a set of shared software systems, standards, and utilities, and the use of such frameworks have recently received considerable attention for hydrological models as well as for more complex Earth system and climate models (Dickonson et al., 2002; Wollheim et al., 2008). Besides the structural changes compared to the previous versions of WBM/WTM (Vörösmarty et al., 1998), the most important new elements in WBM<sub>plus</sub>

## Reconstructing 20th century global hydrography

D. Wisser et al.

Title Page

Abstract

Introduction

Conclusions

References

Tables

Figures

◀

▶

◀

▶

Back

Close

Full Screen / Esc

Printer-friendly Version

Interactive Discussion



are modules that explicitly account for the human activities such as irrigation water abstractions (Wisser et al., 2008) and reservoir operation directly affecting the water cycle processes.

## 2.2 Water balance calculations

- 5 The water balance calculations representing vertical water exchange between the atmosphere and the land surface are performed for rain-fed and irrigated areas separately. Each grid cell is partitioned into irrigated and non-irrigated parts and the water budget over the whole cell is computed as the area weighted average of the two parts.

### 2.2.1 Snowpack

- 10 WBM<sub>plus</sub> implements an improved snowpack simulation over previous versions. The snowpack is calculated uniformly over irrigated and non-irrigated areas. Precipitation is considered snow if the daily mean air temperature is below  $-1^{\circ}\text{C}$  and rain above that threshold. The snow accumulates during the snowing period without allowing sublimation. During the melting periods when snow is on the ground and the temperature is  
 15 above a snowmelt threshold ( $1^{\circ}\text{C}$ ), the snowmelt  $M_s$  [ $\text{mm d}^{-1}$ ] is computed as function of mean daily temperature  $T_m$  [ $^{\circ}\text{C}$ ] and daily precipitation  $P$  [ $\text{mm d}^{-1}$ ] (Willmott et al., 1985):

$$M_s = 2.63 + 2.55T_m + 0.0912T_m P \quad (1)$$

### 2.2.2 Soil moisture balance

- 20 The daily soil moisture budget for the non-irrigated part of the grid cell is given by the original WBM/WTM formulation:

$$dW_s/dt = \begin{cases} -g(W_s) (E_p - P_a) & P_a - E_p \\ P_a - E_p & E_p < P_a \leq D_{WS} \\ D_{WS} - E_p & D_{WS} < P_a \end{cases} \quad (2)$$

2683

## Reconstructing 20th century global hydrography

D. Wisser et al.

Title Page

Abstract

Introduction

Conclusions

References

Tables

Figures

◀

▶

◀

▶

Back

Close

Full Screen / Esc

Printer-friendly Version

Interactive Discussion



where  $g(W_c)$  is a unitless soil, given by

$$g(W_s) = \frac{1 - e\left(-\alpha \frac{W_s}{W_c}\right)}{1 - e^\alpha} \quad (3)$$

and  $W_s$  [mm] is the soil moisture,  $E_p$  [ $\text{mm d}^{-1}$ ] is the potential evapotranspiration,  $P_a$  [ $\text{mm d}^{-1}$ ] is the precipitation available for soil moisture recharge (rainfall  $P_r$  plus snowmelt  $M_s$ ), and  $D_{ws}$  [mm] is the soil moisture deficit to fill soil to its capacity and satisfy  $E_p$ .  $W_c$  [mm] is the soil and vegetation-dependent available water capacity and  $\alpha$  is an empirical constant (set to 5.0).

### 2.2.3 Irrigation water demand

The irrigation water demand in the irrigated fraction of the grid cell is computed for individual crops, distributed globally using global data sets of croplands and aggregated crop types (see Sect. 3.2). The approach implemented in  $\text{WBM}_{\text{plus}}$  to estimate crop evapotranspiration for irrigated crops is the crop coefficient method described in FAO's Irrigation and Drainage Paper 56 (Allen et al., 1998). This method computes crop evapotranspiration  $ET_c$  [ $\text{mm d}^{-1}$ ] as the product of reference evapotranspiration  $ET_0$  [ $\text{mm d}^{-1}$ ] and a crop coefficient  $k_c$ . The crop coefficient represents crop physiological parameters and varies with time. A simple soil moisture balance, taking into account precipitation and crop evapotranspiration is kept and irrigation water  $I_{\text{net}}$  [ $\text{mm d}^{-1}$ ] is applied such that the soil water is refilled to its holding capacity whenever the soil moisture drops below a crop-dependent critical threshold. Rice irrigation is conceptualized by assuming that an additional amount of water is needed to maintain a constant water layer (50 mm) throughout the growing season, and that water percolates at a constant rate into the groundwater. Daily percolation for paddy rice depends on the grid cell soil drainage class (FAO/UNESCO, 2003) and we estimated those rates between  $8 \text{ mm d}^{-1}$  for "extremely well drained soils" and  $2 \text{ [mm d}^{-1}]$  for "very poorly drained soils". The gross irrigation water requirements  $I_{gr}$  [ $\text{mm d}^{-1}$ ] (i.e. the amount of water that actually

## Reconstructing 20th century global hydrography

D. Wisser et al.

Title Page

Abstract

Introduction

Conclusions

References

Tables

Figures

◀

▶

◀

▶

Back

Close

Full Screen / Esc

Printer-friendly Version

Interactive Discussion



has to be extracted from external water resources) is computed by adjusting the net irrigation demand by the irrigation efficiency  $E[-]$  that represents the water losses during irrigation water distribution and the application on the field scale:

$$I_{gr} = \frac{I_{net}}{E} \quad (4)$$

5 To determine the onset of the growing season in the temperate zone, we used a simple temperature threshold and assumed that the growing season starts when the mean monthly air temperature is above 5°C. In areas where crop growth not limited by temperature constraints, we determined the wet (or wettest) season based on the monthly values of the climatological rainfall record and assumed that the growing season starts  
10 one month before the the month with the maximum rainfall in a given year. If multiple cropping is possible, the second season is assumed to start 150 days after the first one.

### 2.3 Runoff retention pool

The excess water  $X_r$  [ $\text{mmd}^{-1}$ ] from the vertical water budget (i.e. the sum of the water surplus that is left after evapotranspiration and soil recharge over rain-fed areas and  
15 return flows from irrigated areas) are partially ( $\gamma X_r$ ) released to the nearby river directly or diverted into the groundwater ( $(1-\gamma)X_r$ ) which is represented as a simple runoff retention pool that delays runoff before it enters the river channel and is described as

$$\frac{dD_r}{dt} = (1 - \gamma) X_r - \beta D_r \quad (5)$$

20 The river runoff becomes

$$R_r = \gamma X_r + \beta D_r \quad (6)$$

where  $D_r$  [ $\text{mm d}^{-1}$ ] is the rainfall runoff detention pool,  $R_r$  [ $\text{mm d}^{-1}$ ] is the runoff from the grid cell,  $\beta$  is an empirical parameter that controls the outflow from the runoff pool

## Reconstructing 20th century global hydrography

D. Wisser et al.

Title Page

Abstract

Introduction

Conclusions

References

Tables

Figures

◀

▶

◀

▶

Back

Close

Full Screen / Esc

Printer-friendly Version

Interactive Discussion



and  $\gamma$  determines the fraction of excess rainfall that fills the pools or becomes runoff instantaneously. The parameter  $\beta$  has units of  $1/T$  and has been set to 0.0167,  $\gamma$  is set to 0.5.

## 2.4 Horizontal water transport

5 The horizontal water transport in  $\text{WBM}_{\text{plus}}$  is only allowed through river systems. FrAMES offers the basic skeleton for flow routing along gridded river networks that propagates water downstream where the actual flow simulation can be carried out by different methods (Döll and Lehner, 2002; Oki and Sud, 1998; Vörösmarty et al., 2000b). For the present study, we applied a Muskingum type solution (Ponce, 1994) 10 of the Saint-Venant flow equations that estimates the outflow  $Q_{j+1}^{t+1}$  [ $\text{m}^3 \text{s}^{-1}$ ] from one grid cell as a linear combination of the inflow  $Q_j^t$  and the outflow  $Q_{j+1}^t$  from the previous time step and the inflow of the current time step  $Q_j^{t+1}$ :

$$Q_{j+1}^{t+1} = C_0 Q_j^{t+1} + C_1 Q_{j+1}^t + C_2 Q_j^t \quad (7)$$

Unit-less coefficients  $C_0$ ,  $C_1$ , and  $C_2$  are parameterized based on riverbed geometry 15 considerations. These coefficients can be expressed as a function of the cell Courant number  $C$  and cell Reynolds number  $C$ :

$$C_0 = \frac{-1 + C + D}{1 + C + D} \quad (8)$$

$$C_1 = \frac{1 + C - D}{1 + C + D} \quad (9)$$

$$C_2 = \frac{1 - C + D}{1 + C + D} \quad (10)$$

20 which are calculated as:

$$C = U_w \frac{\Delta t}{\Delta l} \quad (11)$$

Title Page

Abstract

Introduction

Conclusions

References

Tables

Figures

◀

▶

◀

▶

Back

Close

Full Screen / Esc

Printer-friendly Version

Interactive Discussion



and

$$D = \frac{Q_m}{W_m S_0 U_w \Delta l}$$

where  $U_w$  [ $\text{m}^3 \text{s}^{-1}$ ] is the characteristic speed of the flood wave propagation,  $\Delta l$  [m] is the river cell length,  $\Delta t$  [s] is the time step length,  $S_0$  [-] is the riverbed slope,  $Q_m$  [ $\text{m}^3 \text{s}^{-1}$ ] and  $W_m$  [m] are mean annual discharge and the corresponding flow width. Considering the Manning or the Chezy flow equation and approximating the riverbed shape with power-function

$$Y = aW^b \quad (12)$$

where  $Y$ [m] and  $W$ [m] are the channel depth and width,  $a$  is a shape coefficient and  $b$  is a shape exponent. The flood wave velocity  $U_w$  is strictly a function of the flow velocity  $U$  [ $\text{m}^3 \text{s}^{-1}$ ] and the shape exponent  $b$ :

$$U_w = U\xi = \left(1 + \frac{bp}{b+1}\right) \quad (13)$$

where  $p$  is the exponent of the hydraulic radius according to the Chezy or Manning equations (1/2 or 2/3 respectively). The power function approximation to the riverbed geometry is consistent with empirical at-site discharge-depth and discharge-width relationships (Dingman, 2007). The reference width  $W_m$  [m] and depth  $Y_m$  [m] at mean discharge  $Q_m$  [ $\text{m}^3 \text{s}^{-1}$ ] are calculated by empirical equations:

$$W_m = \tau Q_m \quad (14)$$

and

$$Y_m = \eta Q_m^\phi \quad (15)$$

where  $\eta$ ,  $\tau$ ,  $\nu$ , and  $\phi$  are empirical constants (set to 0.25, 0.40, 8.0, and 0.58 respectively (Knighton, 1998).

## Reconstructing 20th century global hydrography

D. Wisser et al.

Title Page

Abstract

Introduction

Conclusions

References

Tables

Figures

◀

▶

◀

▶

Back

Close

Full Screen / Esc

Printer-friendly Version

Interactive Discussion



## 2.5 Reservoirs

Our implementation of reservoir operations distinguishes two kinds of impoundments: (a) “large” reservoirs for river flow control that directly alter the discharge in river channels and (b) “small” reservoirs for local water management that act as an additional storage pool providing water resources for irrigation. Large river flow control reservoirs are represented explicitly by their position in the simulated river network and their impact on discharge is expressed via flow regulation functions that calculate the outflow at the reservoir location as a function of inflow and reservoir storage. Small water management reservoirs are expressed as lumped storage within grid cells that withhold some of the runoff generated on the non-irrigated portion and release it later to supply irrigation water demand.

### 2.5.1 Large reservoirs

Reservoir operation rules for large scale hydrological models have previously been derived from the main purpose of the reservoir (Haddeland et al., 2006b; Hanasaki et al., 2006). While such an approach is suitable for single reservoirs, applicability on a global scale is a major concern, since the main water management objective for individual reservoirs is not always known and large reservoirs typically serve several purposes. We used a simple relationship of reservoir inflow  $I_t$  [ $\text{m}^3 \text{s}^{-1}$ ] and long-term mean inflow  $I_m$  [ $\text{m}^3 \text{s}^{-1}$ ] to determine the reservoir release  $R_t$  [ $\text{m}^3 \text{s}^{-1}$ ] as

$$R_t = \begin{cases} \kappa I_t & I_t \geq I_m \\ \lambda I_t (I_t - I_m) & I_t < I_m \end{cases} \quad (16)$$

where  $\kappa$  (set to 0.16) and  $\lambda$  (set to 0.6) are empirical constants that have been found by analyzing operational data from some 30 reservoirs globally. Neglecting evaporation from the reservoir surface, the storage  $S_t$  [ $\text{m}^3$ ] in the reservoir can then be described as

$$S_t = S_{t-1} + (I_r - R_t)\Delta t \quad (17)$$

## Reconstructing 20th century global hydrography

D. Wisser et al.

Title Page

Abstract

Introduction

Conclusions

References

Tables

Figures

◀

▶

◀

▶

Back

Close

Full Screen / Esc

Printer-friendly Version

Interactive Discussion



## 2.5.2 Small reservoirs

The number of small reservoirs (not counting innumerable small farm ponds) could be as high as 800 000 (McCully, 1996) but their combined storage capacity is significantly less than the total installed reservoir volume in large reservoirs. The small reservoirs still play a significant role in providing the water resources needed for irrigation. Small reservoirs intercept local runoff from the non-irrigated areas during the wet season and make it available for irrigation during the cropping period. The storage capacity of such runoff harvesting systems is typically computed with reference to the total irrigation requirement and the amount of runoff available for storage (Srivastava, 2001). WBM<sub>plus</sub> estimates the total capacity of small reservoirs in each grid cell by accumulating the water required for irrigation and the available surface runoff over one year as

$$C_{sr} = \min \left( \sum \gamma \mu X_r, \sum I_{gr} \right) \quad (18)$$

where  $\mu$  is a correction factor that describes the fraction of the excess surface runoff that can be actually stored in the reservoirs, and  $X_r$  and  $I_{gr}$  are the model estimates of surface runoff (Eq. 6) and irrigation water demand (Eq. 4). The factor  $\mu$  depends on a number of local characteristics including topography, land use, geology, and the temporal distribution of rainfall and should be minimized to keep runoff harvesting efficient and effective. For the present study, we assumed that the catchment area for small reservoirs does not exceed the area equipped for irrigation supplied by that area by a factor of 10 based on design recommendations and case studies from a number of regions (Critchley et al., 1991; Srivastava, 1996, 2001). For simplicity, we assumed that small reservoirs in this study have a rectangular cross section and a constant depth of  $h=2$  m. Daily evaporation  $ET$  [ $\text{mmd}^{-1}$ ] from small reservoirs as computed as  $ET = \sigma ET_0$ , where  $\sigma$  is an evaporation coefficient that has been set to 0.6 (Arnold and Stockle, 1991).

## Reconstructing 20th century global hydrography

D. Wisser et al.

Title Page

Abstract

Introduction

Conclusions

References

Tables

Figures

◀

▶

◀

▶

Back

Close

Full Screen / Esc

Printer-friendly Version

Interactive Discussion



## 2.6 Irrigation water uptake

The estimated irrigation water withdrawal requirement  $I_{gr}$  [mm] can be met (in order) by (1) using locally stored runoff from small reservoirs  $W_{SR}$  [mm], (2) by abstracting water from active groundwater (the runoff detention pool  $D_r$ ) (Eq. 5)  $W_{GW}$  [mm], or by

5 (3) abstracting water from local discharge  $Q_j^t$  (Eq. 7) ( $W_{Dis}$ ) [mm], so that the flow in the river is corrected for water abstractions  $W_{dis}$ :

$$Q_{j+1}^{t+1} = C_o Q_j^{t+1} + C_1 Q_{j+1}^t + C_2 Q_j^t - W_{dis} \quad (19)$$

In cases where the demand cannot be met by any one of the three sources, water is still supplied at the required rate, by assuming abstractions will be from groundwater

10 systems that are not hydrologically connected to the system (i.e. fossil groundwater resources).

## 3 Data

### 3.1 Climate data

Monthly atmospheric forcing data (mean air temperature and precipitation) for the pe-

15 riod 1901 to 2002 was obtained from the CRU TS 2.1 data set (Mitchell and Jones, 2005), which represents observed gridded climate data at a spatial resolution of 30 min (longitude  $X$  latitude) and has been widely used for continental and global scale hydro-

20 logical modeling. This product is not corrected for the effects of errors in gauge-based measurement of precipitation and significant spatial differences between this product and climate model output data are evident at high latitudes where gauge under catch of solid precipitation and under-representation of precipitation at higher elevations intro-

duce a significant bias on observations (Adam et al., 2006; Tian et al., 2007). Correcting the observed precipitation data sets for those effects could increase the terrestrial precipitation by almost 12% (Adam et al., 2006). The CRU precipitation data shows an

Title Page

Abstract

Introduction

Conclusions

References

Tables

Figures

◀

▶

◀

▶

Back

Close

Full Screen / Esc

Printer-friendly Version

Interactive Discussion



increase in precipitation of 2% globally over the last century (Hulme et al., 1998). Most of the increase in annual precipitation is seen in the northern latitudes, Eastern South America, and Central and Northern Australia. Significant declining trends are observed in Western Africa, Northern Africa, Western South America, and Southern East Asia.

### 5 3.1.1 Generating daily precipitation

The non-linearities in system behavior in hydrological processes are particularly relevant with respect to precipitation and the use of monthly or daily precipitation data can lead to significant differences in modeled vertical fluxes (Federer et al., 2003; Vörösmarty et al., 1998). Since the WBM<sub>plus</sub> model is operated at a daily steps, a mechanism was needed to downscale the globally available time series of monthly precipitation inputs to daily values.

We tested two approaches. The first one employed a statistical “weather generator” to create daily rain events by modeling the sequence of wet and dry days within a month based on empirical relationships between monthly rainfall and the number of rainy days and distributing the monthly totals over the wet days such that the daily precipitation amounts follow a gamma distribution (Geng et al., 1986).

The major disadvantage of the weather generator approach was that the spatial correlation of precipitation between neighboring grid cells is “lost” since the daily rain events were generated for each grid cell individually.

The second approach was distributing the monthly values using daily precipitation fraction derived from one degree daily (1DD) precipitation product from Global Precipitation Climatology Project GPCP (Huffman et al., 2001) that is available for the period 1997 to present. We assumed that the differences in the distribution of daily rainfall between years are small and used the daily rainfall values for the year 2002 to rescale the monthly data for the entire CRU record.

We tested the difference between the two approaches and we found that the resulting differences in model predictions were small. As the second approach leads to a more realistic spatial pattern of precipitation we decided to use the daily fraction derived from

## Reconstructing 20th century global hydrography

D. Wisser et al.

Title Page

Abstract

Introduction

Conclusions

References

Tables

Figures



Back

Close

Full Screen / Esc

Printer-friendly Version

Interactive Discussion



the GPCP product.

### 3.2 Agricultural data sets

To create time-varying data sets of irrigated areas for the last century, we used the University of Frankfurt/FAO Global Map of Irrigated Areas (Siebert et al., 2005b; Siebert et al., 2005a) that shows the “areas equipped for irrigation” around the year 2000 at a spatial resolution of 5 arc minutes (around 8 km at the equator) and is based on irrigation statistics from sub-national and national statistics and a variety of atlases and other sources. We rescaled the values in each grid cell on a country-by-country basis using the time series of irrigated areas per country recently compiled from national statistics by (Freydank and Siebert, 2008). Despite significant uncertainties (in particular for the first half of the last century), and the inability to map changes in the distribution of irrigated areas within a country, this data set adequately reflects the large-scale dynamics of the development of irrigated area over the last century, with an expansion of areas equipped for irrigation from just over 53 Mha in 1901 to 285 Mha in 2002. It is important to note that not all areas “equipped for irrigation” will actually be irrigated in any given year due to market, conditions, the availability of water, and other local conditions. As the actually irrigated areas are not known for most regions, we assumed that all areas equipped for irrigation were actually irrigated. To model the distribution of crops in irrigated areas, we used the dataset by (Monfreda et al., 2008) that shows the distribution of 175 distinct crops across the world in the year 2000 at a spatial resolution of 5 arc minutes and has been derived by synthesizing satellite-derived land cover data and national and international census data. We aggregated the crops into 4 groups (perennial, vegetables, rice, others), determined average values of  $k_c$  from (Allen et al., 1998), and assumed a constant distribution of crops in each irrigated grid cell over the entire simulation period. Both data sets have been aggregated to match the resolution of the 30 min river network. Irrigation efficiency data (i.e. the fraction of water actually used by the crop related to the water abstracted from sources) has been taken from the country averaged numbers provided by (AQUASTAT, 2008) and

## Reconstructing 20th century global hydrography

D. Wisser et al.

Title Page

Abstract

Introduction

Conclusions

References

Tables

Figures

◀

▶

◀

▶

Back

Close

Full Screen / Esc

Printer-friendly Version

Interactive Discussion



(Döll and Siebert, 2002). Irrigation intensity (defined as the total area of harvested crops over the total irrigated area) was derived from (AQUASTAT, 2008). Soil hydraulic properties to determine the soil moisture holding capacity in both, non-irrigated and irrigated fractions of the grid cell have been taken from the UNESCO/FAO soil map of the world (FAO/UNESCO, 2003).

### 3.3 Hydrography data

#### 3.3.1 River network

To link the terrestrial land mass to the oceans and to route the modeled runoff, we used the Simulated Topological Network (STN) of gridded rivers at 30-min spatial resolution (Vörösmarty et al., 2000a, b) that organizes the terrestrial land mass of the continents into 6192 river basins with catchment size ranging from  $10^3$  to  $5.9 \times 10^6$  km<sup>2</sup>.

#### 3.3.2 Reservoirs

River flow regulating (“large”) reservoirs are represented as points along the simulated gridded network where WBM<sub>plus</sub> applies simple reservoir operation rules adjusting the incoming flow (Sect. 2.4) to simulate water release from the reservoir. Location and attributes of the existing reservoirs were taken from the global repository of registered impoundments (Vörösmarty et al., 1997, 2003) that reports reservoirs with a maximum storage capacity of more than 0.5 km<sup>3</sup> and contains 668 reservoirs from the International Commission on Large Dams (ICOLD) registry of dams (ICOLD, 1998, 2003). The combined contemporary maximum capacity for those reservoirs was 4726 km<sup>3</sup> and represents 67% of the total volume of impoundments formed by dams over 15 m. Reservoirs were co-registered to the STN-30 river network ensuring that reservoirs are located on main tributaries. Reservoirs sharing the same grid cell were collapsed into single reservoir with the sum of capacities of the individual reservoirs. The year of construction given in the ICOLD database was used to create a time-varying data set

## Reconstructing 20th century global hydrography

D. Wisser et al.

Title Page

Abstract

Introduction

Conclusions

References

Tables

Figures

◀

▶

◀

▶

Back

Close

Full Screen / Esc

Printer-friendly Version

Interactive Discussion



of reservoir capacities.

## 4 Model simulations

Model simulations for the last century were performed for two different configurations. First, we computed the components of the hydrological cycle under “pre-managed” conditions, i.e. the reservoir and the irrigation water modules were turned off. The second configuration simulated disturbed conditions using the time varying agricultural data sets described above to estimate irrigation water demand and water withdrawals plus the reservoir routing for any existing reservoirs.

We did not account for the interactions of atmospheric CO<sub>2</sub> concentrations with the hydrological cycle through reduced transpiration per unit leaf and thus increasing runoff (Betts et al., 2007). Furthermore, we did not investigate the effects of land use changes (most notably deforestation) that have been shown to have significant impacts on the hydrological cycle (Gordon et al., 2005; Haddeland et al., 2007; Piao et al., 2007) and have been shown to increase runoff globally (Piao et al., 2007) at the same order of magnitude as the changes imposed by increased evapotranspiration in irrigated areas (Gordon et al., 2005). We do not consider the potential contribution of melting of permafrost areas and glaciers on continental runoff.

Daily potential evapotranspiration was computed using the Hamon relationship (Hamon, 1963) as a function of daily mean air temperature and the length of the day and taken as reference evapotranspiration  $ET_0$  [mm] to compute crop water demand in irrigated areas:

$$ET_0 = \frac{715.5\Lambda e_s T_m}{T_m + 273.2} \quad (20)$$

Where  $\Lambda$  [-] is the daylength (expressed as a fraction of a 24 h period), and  $e_s$  [kPa] is the saturation water pressure at the mean air temperature  $T_m$  [°C].

## Reconstructing 20th century global hydrography

D. Wisser et al.

Title Page

Abstract

Introduction

Conclusions

References

Tables

Figures

◀

▶

◀

▶

Back

Close

Full Screen / Esc

Printer-friendly Version

Interactive Discussion



It is important to note that in keeping with earlier approaches (Federer et al., 2003; Vörösmarty et al., 1998) the model parameters in the WBM<sub>plus</sub> model were assigned a priori and not further calibrated to match observed discharge.

## 5 Results and discussion

### 5.1 Model validation

Previous versions of the WBM/WTM model were validated against discharge records in various geographical regions (e.g. conterminous US by Vörösmarty et al., 1998), Amazon by Vörösmarty et al., 1996 and globally by Fekete et al., 2002. All previous studies showed that WBM/WTM had little bias (<4% on observed runoff when applied to the conterminous US) over large domains while individual basins could have large discrepancies. For the present study we validated predicted time series of simulated discharge against the same set of discharge gauges from the Global Runoff Data Centre (GRDC) that were used in previous work by (Fekete et al., 2002) in developing UNH-GRDC Composite Runoff Fields (Fekete et al., 1999, 2002). The selected 663 stations monitor 52% of the continental land mass (excluding Antarctica) and 70% of the continental discharge to oceans (Fekete et al., 2002). The period of observation varies greatly between stations with a peak in data availability in the 1980's. We further reduced the number of stations by including only those stations that have a minimum length of record of 10 years. The number of observation-months for the final selection of 660 stations ranges from 120 to 1224 (mean 541, median 477) months. Model performance was assessed using the Mean Bias Error (MBE), computed as the sum of the differences of predicted values  $P_i$  minus observed values  $O_i$  divided by the number of observations, the mean absolute error (MAE), computed as the sum of the absolute differences between  $P_i$  and  $O_i$  over the number of observations, and the Index of

## Reconstructing 20th century global hydrography

D. Wisser et al.

Title Page

Abstract

Introduction

Conclusions

References

Tables

Figures

◀

▶

◀

▶

Back

Close

Full Screen / Esc

Printer-friendly Version

Interactive Discussion



agreement  $d_j$  (Willmott, 1981), given by:

$$d_j = 1 - \frac{\sum_{i=1}^n |O_i - P_i|^j}{\sum_{i=1}^n (|P_i - \bar{O}| + |O_i - \bar{O}|)^2} \quad (21)$$

where  $j$  represents an arbitrary positive integer value (set to  $j=2$ ) and  $d_j$  ranges from zero (poor model) to 1.0 (perfect model).

Figure 1 shows the frequency distribution of the mean monthly bias and the  $d$ -statistics for the selected stations for model simulations under disturbed conditions from 1901–2002. Despite significant differences between simulated and observed discharge at some gauging stations, the low bias reaffirms our findings regarding WBM's low bias when applied over large spatial domains. Averaged for all stations, the average MBE of  $-1.2 \text{ mm month}^{-1}$  indicates that the model on average underestimates discharge and this negative bias can partly be explained with biases arising from errors in the precipitation input fields due to gauge undercatch (Sect. 3.1.1). As the bias arising from uncertainties in the input data partly cancels out over large domains, the model performance generally increases with basin size (Hunger and Döll, 2007; Fekete et al., 2002).

## 5.2 Irrigation water withdrawal

The simulated amount of water that needs to be abstracted from groundwater, small reservoirs, and rivers globally based on the time-varying data set of irrigated areas described above increased from  $590 \text{ km}^3 \text{ a}^{-1}$  in 1901 to  $2997 \text{ km}^3 \text{ a}^{-1}$  for the year 2002. The contemporary withdrawal compares to previous estimates based on the the same contemporary distribution of irrigated areas that range from  $2200 \text{ km}^3 \text{ a}^{-1}$  to around  $3000 \text{ km}^3 \text{ a}^{-1}$  (Döll and Siebert, 2002; Hanasaki et al., 2007; Siebert and Döll, 2007; Vörösmarty et al., 2005). By continents, most the withdrawal is estimated for Asia

Title Page

Abstract

Introduction

Conclusions

References

Tables

Figures

◀

▶

◀

▶

Back

Close

Full Screen / Esc

Printer-friendly Version

Interactive Discussion



(~83%), home to most of the worlds rice paddies and multiple cropping (Maclean et al., 2002). Irrigation water withdrawal in North America (~6% of the total) increased sharply between 1940 and 1950 (Fig. 2). With the exception of Europe (~3% of the global withdrawal), all continents show a steady upward trend over the last 100 years in irrigation water use reflecting the expansion of irrigated areas (Sect. 3.2).

As the withdrawal of water for irrigation will have different impacts on components of the hydrological cycle, as well as biogeochemical fluxes, depending on the source where it is taken from, it is important to know if the water is supplied by groundwater or surface water. Although some estimates exists on the global scale, a detailed, consistent inventory of this information is lacking (Oki and Kanae, 2006). The fraction of irrigation that is supplied by groundwater varies greatly within regions. US agriculture, for example, relies on 65% groundwater (Pimentel et al., 2004), while groundwater is supplying an estimated 50% to 60% in India (Singh and Singh, 2002; Thenkabail et al., 2006), and 40% in China (Thenkabail et al., 2006). Foster and Chilton (2003) compiled data on irrigation water use for selected countries and concluded that the contribution of groundwater to irrigation water abstractions is approaching 30% globally.

The  $WBM_{plus}$  computed estimates for the contribution of discharge from rivers and the runoff detention pool  $D_r$  are 10% and 17%, respectively and 33% being supplied from locally stored runoff in small reservoirs (Table 1). As noted earlier, cases can occur where the demand cannot be met by either locally produced runoff or river corridor discharge, representing the mining of fossil groundwater. Our estimates of the volume of water that has to be abstracted from those non-renewable sources increased from  $220 \text{ km}^3 \text{ a}^{-1}$  in 1901 to  $1200 \text{ km}^3 \text{ a}^{-1}$  under contemporary conditions, representing 40% of the estimated global agricultural water withdrawal. While this estimate is consistent with earlier estimates of the unsustainable water use (Vörösmarty et al., 2005), it may represent an overestimation as  $WBM_{plus}$  does not represent the dynamics of large groundwater systems from which water can be withdrawn in areas far away from the areas where the system is recharged. This lack of an adequate representation of deeper groundwater is a key shortcoming of current macroscale hydrology

## Reconstructing 20th century global hydrography

D. Wisser et al.

Title Page

Abstract

Introduction

Conclusions

References

Tables

Figures

◀

▶

◀

▶

Back

Close

Full Screen / Esc

Printer-friendly Version

Interactive Discussion



models (Lettenmaier, 2001). Over the last century, the total accumulated volume of non-renewable water abstractions is  $55\,639\text{ km}^3\text{ a}^{-1}$ , representing about half of the total precipitation reaching the Earth's surface in one year. The total water withdrawn from non-renewable water resources represents only about 0.2% the volume of water currently stored in all groundwater stocks, estimated to be  $23\times 10^6\text{ km}^3$  (Oki and Kanae, 2006).

### 5.3 Spatial trends in hydrological components

To assess spatial patterns of trends in predicted components of the hydrological cycle over the last century, we computed trends of the predicted annual values of evapotranspiration and runoff for each grid cell under natural and disturbed conditions. Under natural conditions, the spatial distribution of the trend in simulated evapotranspiration over the last century reflects the variations in the temperature and precipitation drivers (Fig. 3). As the temperature shows an upward trends for almost all regions, the trends in evapotranspiration for individual continents are dominated by increases or decreases in available water and hence by the increases or decreases in the precipitation data. Increases in evapotranspiration are seen in the mid to high latitude regions, Central Southern Africa, Eastern South America, and Central Australia.

Under disturbed conditions, the expansion of irrigated areas over the last century has significantly increased evapotranspiration in Eastern China, the India, Central America, and Central Asia. Negative trends in predicted evapotranspiration reflect the changes in precipitation and can be seen in Western and Central Africa, Western South America, and parts of South East China.

Predicted changes in evapotranspiration and trends in the precipitation input data result in increases in the predicted runoff (precipitation – evapotranspiration) in the high latitude regions, Eastern South America, Northern Australia, and mid-latitude North America and runoff decreases in Western Africa, Argentina, Eastern China, and parts of Central Asia (Fig. 4). The general pattern of the spatial distribution of runoff trends is consistent with the global distribution the of significant trends in observed discharge

## Reconstructing 20th century global hydrography

D. Wisser et al.

Title Page

Abstract

Introduction

Conclusions

References

Tables

Figures

◀

▶

◀

▶

Back

Close

Full Screen / Esc

Printer-friendly Version

Interactive Discussion



for the period 1971–1998 compared to 1901 to 1970 (Milliman et al., 2008; Milly et al., 2005) and observed increases in North America (e.g. Qian et al., 2007). Changes in evapotranspiration imposed by the expansion of irrigated areas and increased evapotranspiration translate to significant decreases in the predicted runoff in Eastern China and India.

## 5.4 Global discharge

The spatial trends in runoff and evapotranspiration described above translate to changes in the predicted terrestrial discharge into the Oceans and to endorheic basin receiving waters (e.g. Aral and Caspian Seas). Based on the basin characteristics given in the STN river network (Sect. 3.3.1) we calculated time series of flow water entering the oceans and endorheic basins and determined the significance of possible trends in those time series at the 0.05 level.

This section will first discuss the total predicted terrestrial discharge over the last century and then the predicted discharge for individual Oceans and from continents reflecting the impact of variations in the climate drivers alone and from changes induced by the expansion of irrigated lands and the operation of reservoirs. The results are compared with earlier estimates by Fekete et al. (2002) that have been derived by combining modeled runoff with observed discharge at 663 river gauging stations. Annual time series of discharge in major endorheic rivers and major rivers draining into the ocean basins for the last century are shown in Fig. 7.

Our estimate of the long term mean annual freshwater export from the terrestrial surface of the Earth (taking into account irrigation water abstractions) for the last century is  $37\,405\text{ km}^3\text{ a}^{-1}$  and is consistent with earlier estimates (Dai and Trenberth, 2002; Döll et al., 2003; Fekete et al., 2002; Sitch et al., 2003; Vörösmarty et al., 2000c, 2005) The estimated annual discharge varies considerably between  $32\,783$  and  $41\,725\text{ km}^3\text{ a}^{-1}$ , a larger range than estimates made by (Shiklomanov and Rodda, 2003) and shows the highest values during the period 1951–1975 (Table 2). The highest value of annual terrestrial discharge ( $41\,725\text{ km}^3\text{ a}^{-1}$ ) represents a  $\sim 12\%$  increase compared to

## Reconstructing 20th century global hydrography

D. Wisser et al.

Title Page

Abstract

Introduction

Conclusions

References

Tables

Figures

◀

▶

◀

▶

Back

Close

Full Screen / Esc

Printer-friendly Version

Interactive Discussion



Reconstructing 20th century global hydrography

D. Wisser et al.

Title Page

Abstract

Introduction

Conclusions

References

Tables

Figures



Back

Close

Full Screen / Esc

Printer-friendly Version

Interactive Discussion



the long-term mean annual value. The minimum annual discharge (in 1992) in the last century is 16% lower than the mean annual value and is related to the substantial decrease in global precipitation following the eruption of Mt. Pinatubo in June 1991 (Trenberth and Dai, 2007). Over the entire simulation period, the global total runoff increases slightly ( $11 \text{ km}^3 \text{ a}^{-1}$  under pristine conditions and  $6 \text{ km}^3 \text{ a}^{-1}$  when the effects of water abstractions for irrigation are taken into account) but both trends are not significant. The flow alteration imposed by the construction of reservoirs over the last century gradually decreased the variability of the estimated discharge expressed by the coefficient of variation (CV) of monthly discharge values and is discussed in more detail in Sect. 5.6.

The increased evapotranspiration over irrigated areas leads to a reduction of terrestrial runoff that is partly offset by the additional water abstracted from groundwater systems that are not connected to the hydrological cycle (Sect. 5.2). Combined, this additional water and increased evapotranspiration leads to a gradual reduction of global discharge ranging from 0.6% at the beginning of the last century to around 2% in 2000.

Despite being insignificant for the total discharge entering the oceans, the hydrologic alterations imposed by the construction of reservoirs and the expansion of irrigated areas may have dramatic effects at the regional scale and thus impact the flow to the oceans or endorheic receiving waters. Table 3 summarizes the characteristics of basins draining into the Oceans and irrigated areas and an overview of the basins and the receiving oceans is given in Fig. 5.

5.4.1 Land/endorheic basins

Major internally draining basins include the Central Asian Drainage basin, the Caspian Sea, the Aral Sea, and major endorheic lakes in Africa. Around 1.45% of the area in those basins is equipped for irrigation and the installed reservoir capacity, expressed as the mean residence time (reservoir capacity over mean annual discharge) is 0.29 (under contemporary conditions).

The estimated annual discharge from those basins shows considerable varia-

Reconstructing 20th century global hydrography

D. Wisser et al.

|                          |              |
|--------------------------|--------------|
| Title Page               |              |
| Abstract                 | Introduction |
| Conclusions              | References   |
| Tables                   | Figures      |
| ◀                        | ▶            |
| ◀                        | ▶            |
| Back                     | Close        |
| Full Screen / Esc        |              |
| Printer-friendly Version |              |
| Interactive Discussion   |              |



tions (between  $774 \text{ km}^3 \text{ a}^{-1}$  and  $1650 \text{ km}^3 \text{ a}^{-1}$  under disturbed conditions) and is  $1037 \text{ km}^3 \text{ a}^{-1}$  on average (Table 2). Discharge in endorheic basins is slightly declining over the entire period, most notably in the last 25 years in of the last century. Over the last century, the trend is negative (but insignificant),  $-0.2 \text{ km}^3 \text{ a}^{-1}$  under pristine conditions and  $-0.5 \text{ km}^3 \text{ a}^{-1}$  taking into account the effects of irrigation water withdrawal.

The construction of reservoirs has lead to a considerable decrease of the variability of monthly flows, most drastically in the period 1975–200, where the coefficient of variation (CV) for monthly discharge has increased from 0.52 to 0.37 (Table 2). Figure 7 exemplarily shows the modeled time series for the Okavango river with high flows during the 1970’s and consecutive dry years in the mid 1980’s.

5.4.2 Ocean receiving waters

*Mediterranean/Black Sea*

The basins draining into the Mediterranean and Black Sea are among the most heavily influenced with regard to the effects of irrigation and reservoirs (Table 3). The discharge to the Black Sea is dominated by the Danube (50%), the Dnepr (15%) and the Don (9%).

The discharge to the Mediterranean is dominated by the flow of the river Nile contributing more than 53% to the total inflow. Other important rivers include the Po (9%) and the Rhone river (7%). Similar to endorheic basins, basins draining into the Mediterranean are experiencing a decline in discharge in the last 25 years of the last century. Over the last century, the trend in discharge under natural conditions is  $-1.2 \text{ km}^3 \text{ a}^{-1}$  (significant) and under disturbed conditions  $-1.4 \text{ km}^3 \text{ a}^{-1}$  (insignificant).

It is important to note, that our modeled discharge under disturbed conditions can be higher than the estimated discharge under natural conditions in very dry years (for example in 1984 and 2000; Fig. 7).

This can largely be explained with the irrigation in grid cells along the Nile river and in the Nile delta that do not fall in the same grid cell as the river and therefore cannot be

supplied by river discharge. As the local runoff in these regions is close to zero, water is primarily supplied from fossil groundwater sources and the return flow from irrigated areas eventually increases runoff.

### ***Atlantic Ocean***

5 About 30% of the terrestrial flow to the Atlantic Ocean is coming from the Amazon river. Other important rivers include the Zaire (9%), Mississippi (4%), and Parana (4%).

Given the large volume of discharge entering the Atlantic Ocean, the effect of human interventions on the discharge volume is negligible small; over the last century, the combined effect of increased evapotranspiration and water withdrawal from non-renewable sources reduces the annual discharge into the Atlantic Ocean by  $33 \text{ km}^3 \text{ a}^{-1}$  (0.2%). The annual flow of the Amazon river shows considerable variations but is not affected by irrigation water abstractions (Fig. 7).

10 Over the last century, discharge into the Atlantic Oceans shows an upward (but insignificant) trend of  $5.4 \text{ km}^3 \text{ a}^{-1}$  and  $5.8 \text{ km}^3 \text{ a}^{-1}$  under pristine conditions and disturbed conditions respectively.

### ***Indian Ocean***

The most important rivers draining into the Indian Ocean are the Ganges (with a flow equivalent to 23% of the total), the Irrawaddy (12%), and the Zambezi (6%). Our estimate of the long-term mean annual discharge entering the Indian Ocean is  $4983 \text{ km}^3 \text{ a}^{-1}$  with significant reductions imposed by the expansion of irrigated areas and increased evapotranspiration in basins draining into the Indian Ocean. With 4% of the drainage area being under irrigation, irrigation water abstraction reduces the total flow to the Indian Ocean by almost 5% averaged over the last century with the a reduction reaching the highest values ( $\sim 7\%$ ) in the last 25 years of the 20th century.

20 Under both disturbed and pristine conditions, the time series show decreasing but insignificant trends ( $-0.14 \text{ km}^3 \text{ a}^{-1}$  and  $-2.0 \text{ km}^3 \text{ a}^{-1}$ ). Figure 7 illustrates the gradual

## Reconstructing 20th century global hydrography

D. Wisser et al.

Title Page

Abstract

Introduction

Conclusions

References

Tables

Figures

◀

▶

◀

▶

Back

Close

Full Screen / Esc

Printer-friendly Version

Interactive Discussion



reduction of discharge under disturbed conditions over the last century for the Ganges river.

### ***Pacific Ocean***

Important rivers draining to the Pacific Ocean include the Chang Jiang (9%), the Mekong (4%) and the Amur (3%). Although areas under irrigation represent ~4% of the drainage area (Table 3), increased evapotranspiration translates only to a reduction of  $341 \text{ km}^3 \text{ a}^{-1}$  representing 2.3% of the discharge under natural conditions (averaged over the entire simulation period). With the expansion of irrigated areas, the reduction of flow gradually increases, with a steep increase in the last half of the last century. The long-term discharge under disturbed conditions ( $9626 \text{ km}^3 \text{ a}^{-1}$ ) varies considerably over the last century. As discharge into the Atlantic, discharge was highest in the 1951–1975 period (~5% higher than averaged over the 20th century). Over the entire simulation period, discharge under natural and disturbed conditions increases by  $2.7 \text{ km}^3 \text{ a}^{-1}$  and  $0.5 \text{ km}^3 \text{ a}^{-1}$ , respectively, both trends being insignificant. Exemplarily, the flow reductions in the Chang Jiang river basin are depicted in Fig. 8.

### ***Arctic Ocean***

Flow into the Arctic Ocean is dominated by the Yenisei, Lena, Ob, Mackenzie rivers, contributing to more than half of the total flow. Owing to the large volumes of spring discharge that is dominated by snow melt compared to summer flows, the variability of streamflow in basins is higher than for any other ocean (CV for monthly values under pristine conditions is around 1.0). Reservoirs are responsible for a substantial change in the seasonality of streamflow in Arctic river basins (Adam et al., 2007), and the construction of reservoirs over the last century has gradually led to a slight reduction of the variability of modeled discharge entering the Arctic Ocean (Table 2). It is noteworthy that our estimate of the long-term mean annual discharge into the Arctic Ocean ( $2282 \text{ km}^3 \text{ a}^{-1}$ ) is around 30% lower than the  $3268 \text{ km}^3 \text{ a}^{-1}$  estimated

## **Reconstructing 20th century global hydrography**

D. Wisser et al.

Title Page

Abstract

Introduction

Conclusions

References

Tables

Figures

◀

▶

◀

▶

Back

Close

Full Screen / Esc

Printer-friendly Version

Interactive Discussion



Reconstructing 20th century global hydrography

D. Wisser et al.

Title Page

Abstract

Introduction

Conclusions

References

Tables

Figures

◀

▶

◀

▶

Back

Close

Full Screen / Esc

Printer-friendly Version

Interactive Discussion



from gauge corrected runoff fields (Fekete et al., 2002) and the  $3200 \text{ km}^3 \text{ a}^{-1}$  estimated based on contemporary discharge records (Serreze et al., 2006). The discrepancy can largely be attributed the huge uncertainties in Arctic hydroclimatological data arising from the sparse network of Arctic climate stations (Rawlins et al., 2006) and gauge under catch, due to the vicinity of gauge locations to highly populated places and the non-representativeness of those gauges of complex topographic features (Adam et al., 2006). Over the last century, we find that discharge into the Arctic Ocean shows a significant positive trend of  $4.2 \text{ km}^3 \text{ a}^{-1}$ . This trend is consistent with the annual rate of increase of  $2.0 \pm 2.7 \text{ km}^3 \text{ a}^{-1}$  that has been estimated from observed discharge from the six Eurasian arctic rivers from 1936–1999 (Peterson et al., 2002) and upward trend of  $8.2 \text{ km}^3 \text{ a}^{-1}$  for the period 1949–2004 that has been found by (Dai et al., 2008) from a new dataset of observed streamflow where missing data was filled by results from simulations of a land surface model.

5.5 Model results for selected river basins

This section is aimed at discussing the simulated discharge at selected river basins and exemplifying the impact of irrigation water management and reservoir operation on simulated monthly hydrographs. Figure 8 shows time series of monthly values (aggregated from daily predictions) of observed and modeled time series under natural and disturbed conditions for selected gauging station representing a wide range of catchment sizes, water management practices and climatic conditions.

Syr Darya and Amu Darya, feeding the Aral Sea in Central Asia are among the most the most prominent examples of heavily impacted river basins. The two basins have undergone significant distortions of their hydrographs due to the expansion of irrigated areas and the construction of reservoirs in the 1960's and 1970's. The abstraction of water for irrigation purposes has lead to the shrinking of the Aral Sea to about half its size and to a reduction of about 90% of its volume (Micklin, 2007).

Two reservoir were constructed upstream of the station at Kal at the Syr Darya river

in the tributaries Naryan river and Kara Narya River in 1978 and 1980 with a combined storage capacity of  $21.75 \text{ km}^3$ . As a result, the hydrograph shows a significant decrease in the variability. The coefficient of variation (CV) for modeled monthly values of discharge for the pre-management period (1950–1969) decreased from 1.2 to 0.52 for the period 1980–1999, and is closer to the CV of observed values (0.44) for the same period.

Similarly, irrigation water use reduces the estimated flow in the Amu Darya at Kerki by 14% and the operation of reservoirs lead to an increase in low flows whereas flows during the wet season are greatly reduced.

The Sebou river, one of the largest rivers in Morocco is heavily influenced by the development of irrigation with natural vegetation covering only 25% of the total catchment area of  $40\,000 \text{ km}^2$  (Snoussi, 2002). The construction of the Idriss 1er dam on the Inaouene tributary in 1973 ( $V=1270 \text{ km}^3$ ) has lead to a remarkable decrease in the variability of the observed flow and a reduction of the total flow of about 55% (Snoussi et al., 2002). While the model simulations under natural conditions for the gauging station at Azib Soltane capture the observed hydrograph reasonably well, the pristine simulations after the construction of the reservoir grossly overestimate the variability and volume of the flow, indicating that the operation of reservoirs need to be taken into account to adequately represent the anthropogenic changes in macroscale hydrological models.

Despite a large storage capacity of reservoirs upstream of the gauging station at Mukdahan ( $8.46 \text{ km}^3$ ), the seasonality of the flow of the Mekong river is not significantly affected by the operation of reservoirs (Haddeland et al., 2006a). The consumptive use for the total area is  $8.2 \text{ km}^3 \text{ a}^{-1}$  and represents a 4% decrease in streamflow, comparable to the previous estimates of water withdrawal for the entire basin of  $13 \text{ km}^3 \text{ a}^{-1}$  (Haddeland et al., 2006a).

Being one of the most heavily regulated river basins in North America with a combined storage capacity of  $76 \text{ km}^3$  in the area upstream of the gauging station The Dalles, reservoir operation and irrigation depletion have greatly affected the river flow

## Reconstructing 20th century global hydrography

D. Wisser et al.

Title Page

Abstract

Introduction

Conclusions

References

Tables

Figures

◀

▶

◀

▶

Back

Close

Full Screen / Esc

Printer-friendly Version

Interactive Discussion



of the Columbia River. The variability of monthly modeled discharge decreased from 0.82 for the first half of the century to 0.46 for the period after 1950 (compared to observed values of 0.70 and 0.43). Water abstraction for irrigation has lowered the flow volume by 2.5% on average during the same period.

5 The flow volume of the North Saskatchewan near Deer Creek is unaffected by irrigation water use but significantly altered by the construction of two reservoirs with a combined capacity of 2.5 km<sup>3</sup>. Variability of monthly flows decreased from around 1.0 in the period before 1970 to 0.52 for period after 1970 and captures the variability of  
10 observed streamflow (0.56) during the same period reasonably well despite differences in the modeled flow volume.

## 5.6 River water aging

Vörösmarty et al. (1997) introduced the concept of river water aging, related to residence time change of river flow through artificial impoundments, to illustrate the impact of the construction of reservoirs on simulated discharge over the last century. It must  
15 not be confused with the true “age” of water molecules that can be determined, for example, using tracer hydrological methods.

We apply here this concept and compute the mean water age of water entering the oceans and endorheic basins under natural and disturbed conditions. The aging of water in its passage to the oceans reflects disturbance in of the natural water cycle and  
20 determines a number of direct and indirect changes in the physical, biogeochemical, and geomorphological processes, such as hydrograph distortion, reaeration capacity, sediment trapping efficiency (Vörösmarty and Sahagian, 2000).

Building on earlier work by (Vörösmarty et al., 1997) and using the river bed parameterization described in equations described in Sect. 2.4, we can estimate the natural  
25 and reservoir-induced residence time  $\tau_m$  [s] of water in each grid cell. Residence time is determined by relating the modeled annual discharge  $Q_m$  [m<sup>3</sup>/s] to the river volume  $V_{riv}$  [m<sup>3</sup>] and reservoir volume  $V_{res}$  (accumulated downstream using the STN-30 net-

## Reconstructing 20th century global hydrography

D. Wisser et al.

Title Page

Abstract

Introduction

Conclusions

References

Tables

Figures



Back

Close

Full Screen / Esc

Printer-friendly Version

Interactive Discussion



work):

$$\tau_m = \frac{uV_{\text{res}} + V_{\text{riv}}}{Q_m} \quad (22)$$

where  $u$  is a utilization factor that relates mean modeled annual storage in each reservoir to the reservoir capacity and  $V_{\text{riv}}$  is the storage volume in the river, computed as  $V_{\text{riv}} = Y_m W_m$  (Eqs. 14 and 15). The computed age varies with the modeled annual discharge and the estimated reservoir storage based on the reservoir operation described in Sect. 2.5.1. Our estimate of the discharge weighted apparent water age globally is 19 days and is consistent with earlier estimates days (Covich, 1993; Vörösmarty et al., 2000b; Vörösmarty et al., 1997). The discharge weighted age of water entering the oceans varies considerably between 8 days for basins entering the Pacific Ocean and 39 days for the Mediterranean basins (Table 4).

The additional water age imposed by the construction of impoundments in the last century as increased the mean water age by 42 days, with the largest increases in  $\Delta\tau_m$  observed in endorheic basins, basins draining to the Mediterranean and basins draining into the Pacific Ocean. The apparent additional aging  $\Delta\tau_m$  shows the most significant increase during the period 1950–1980 when the construction of large reservoirs has reached its peak and flattens out after the 1980's (Fig. 10). The differences in the apparent aging under natural and disturbed conditions are depicted in Fig. 9.

These changes have a number of direct and indirect effects on the temporal distribution of discharge, biogeochemical processes in the river and geomorphologic process. For example, the construction of reservoirs has been shown to result in significant losses in sediments in the coastal zone (Vörösmarty et al., 2003, 2007) and thereby influences the effective sea level rise in a number of highly populated deltas, including the Nile, Ebro, Volta, and Niger (Vörösmarty et al., 2007).

## Reconstructing 20th century global hydrography

D. Wisser et al.

Title Page

Abstract

Introduction

Conclusions

References

Tables

Figures

◀

▶

◀

▶

Back

Close

Full Screen / Esc

Printer-friendly Version

Interactive Discussion



## 6 Summary and conclusions

Using a water balance and transport model with time series of climate drivers we have reconstructed the hydrography of terrestrial discharge for the last century, explicitly accounting for the effects of human interventions in the hydrological cycle. To separate the effects of human engineering and the climate drivers alone, model simulations were performed for disturbed and natural conditions. The good agreement between observed and predicted discharge at a large number of gauging stations globally indicates that the model simulations, forced with time-varying geospatial data sets of irrigated areas and reservoirs reasonably well reproduces the variations in components of the hydrological cycle caused by the climate drivers and the anthropogenic changes. The approach can therefore potentially be used to help understanding the role of human interventions in continental and global water cycles for near-real time predictions and future scenarios of those drivers.

The results for individual river basins suggest a reduction of flow as a result of the expansion of irrigation and changes in the seasonality of flow imposed by the operation of reservoirs. These results are in general agreement with previous observations (Bouwer et al., 2006; Haddeland et al., 2006a) and highlight the need to account for human interventions in the water cycle in macroscale hydrological models. The changes in the hydrological cycle in river basins with a large fraction of the basin area under irrigation have been shown to be governed by the impact of human engineering rather than changes in the climate signal. Despite being dramatic for individual river basins, the annual discharge entering the oceans is governed by variations in the climate forcings over the last century and is not significantly altered by water abstractions for irrigation (Dai et al., 2008; Milliman et al., 2008).

Under natural conditions, we find significant decreasing trends ( $-1.2 \text{ km}^3 \text{ a}^{-1}$ ) of the flows entering the Mediterranean and Black Sea and significantly increasing discharge ( $4.2 \text{ km}^3 \text{ a}^{-1}$ ) to the Arctic Ocean.

With the exception of the Arctic Ocean, we do not find significant trends in modeled

**HESSD**

6, 2679–2732, 2009

### Reconstructing 20th century global hydrography

D. Wisser et al.

Title Page

Abstract

Introduction

Conclusions

References

Tables

Figures

◀

▶

◀

▶

Back

Close

Full Screen / Esc

Printer-friendly Version

Interactive Discussion



time series of accumulated streamflow entering the major ocean basins and endorheic receiving waters over the last century, consistent with previous reports (Dai et al., 2008; Milliman et al., 2008) and contradicting the notion of increasing global runoff as a result of global warming (Labat et al., 2004).

5 The construction of large reservoirs over the last century has gradually and significantly altered the seasonality of streamflow and the dynamics of horizontal water transport in the network of rivers. Using the water aging concept as an indicator to describe the impact of reservoirs on the horizontal transport we found a 300% increase of the apparent water age that, in turn, impacts a number of biogeochemical, geomorphological, and physical processes.

10 Our estimates of components of the hydrological cycle under pristine and disturbed conditions are constrained by a number of uncertainties in the input data as well as uncertainties related to the model itself.

We also recognize the difficulties in separating the effects of changes in the hydrological cycle caused by natural and anthropogenic factors using the simple method presented here because of the interrelated links among climate, atmosphere, soil, and vegetation dynamics (Piao et al., 2007). For example, it is possible that irrigated areas deliver an additional amount of precipitation (Moore and Rojstaczer, 2001) so that the observed rainfall already contain an anthropogenic signal.

20 With regard to the distortion of hydrographs due to the operation of reservoirs, our results are constrained by the incomplete global repository of registered reservoirs (Vörösmarty and Sahagian, 2000). Although the dataset of large reservoirs represents an estimated 67% of the total storage volume of impoundments formed by dams over 15 m, river flow is significantly impacted by the operation of smaller reservoirs that are not accounted for in our model but collectively have a significant impact on river flow and sediment retention (Vörösmarty et al., 2003). Presumably, such uncertainties will gradually be reduced with the development of more accurate, consistent and comprehensive global inventories of dams and reservoirs in combination with high resolution global river networks that are only emerging (Lehner et al., 2008). With regard to the

## Reconstructing 20th century global hydrography

D. Wisser et al.

Title Page

Abstract

Introduction

Conclusions

References

Tables

Figures

◀

▶

◀

▶

Back

Close

Full Screen / Esc

Printer-friendly Version

Interactive Discussion



estimated fraction of the water supplied from non-renewable sources, uncertainties arise from an inadequate representation of large groundwater systems and the lack of a global repository of inter-basin water transfers.

The significance of uncertainties in precipitation on a global-scale water balance context has been previously shown (Fekete et al., 2004). Uncertainties in the precipitation datasets typically translate to higher relative errors in runoff in semiarid regions and the use of different precipitation data sets may therefore lead to different spatial and temporal trends in the hydrological variables.

Future applications of the model will therefore address some of the uncertainties related to the precipitation drivers by using purely satellite based precipitation products such as the Tropical Rainfall Measuring Mission (TRMM), the Global Precipitation Climatology Project 1 degree daily data set (GPCP, Huffman et al., 2001), and blended satellite/gauge based precipitation products such as the GPCP Version 2 product (Adler et al., 2003).

*Acknowledgements.* Observed discharge data has been provided by the Global Runoff Data Centre (GRDC) in Koblenz, Germany. Funding was provided by the NASA Applied Earth Sciences Program through Cooperative Agreement NNA06CN09A and the NASA IDS program (NNX07AH32G).

The presented simulations are part of the Global Terrestrial Network for Hydrology (GTN-H) effort by the World Meteorological Organization that is an effort to establish water cycle monitoring capabilities. The results, together with a number of supplementary model predictions (both historically and near-real time) and data products are available to the scientific community through the GTN-H website (<http://www.gtn-h.net>).

## References

- Adam, J. C., Clark, E. A., Lettenmaier, D. P., and Wood, E. F.: Correction of global precipitation products for orographic effects, *J. Climate*, 19, 15–38, 2006.
- Adam, J. C., Haddeland, I., Su, F., and Lettenmaier, D. P.: Simulation of reservoir influences on

## Reconstructing 20th century global hydrography

D. Wisser et al.

Title Page

Abstract

Introduction

Conclusions

References

Tables

Figures

◀

▶

◀

▶

Back

Close

Full Screen / Esc

Printer-friendly Version

Interactive Discussion



## Reconstructing 20th century global hydrography

D. Wisser et al.

Title Page

Abstract

Introduction

Conclusions

References

Tables

Figures

◀

▶

◀

▶

Back

Close

Full Screen / Esc

Printer-friendly Version

Interactive Discussion



annual and seasonal streamflow changes for the Lena, Yenisei, and Ob' rivers, *J. Geophys. Res.-Atmos.*, 112, D24114, doi:10.1029/2007JD008525, 2007.

Adler, R. F., Huffman, G. J., Chang, A., Ferraro, R., Xie, P., Janowiak, J., Rudolf, B., Schneider, U., Curtis, S., Bolvin, D., Gruber, A., Susskind, J., and Arkin, P.: The Version 2 Global Precipitation Climatology Project (GPCP) Monthly Precipitation Analysis (1979-Present), *J. Hydrometeorol.*, 4, 1147–1167, 2003.

Allen, R. G., Pereira, L. S., Raes, D., and Smith, M.: Crop Evapotranspiration: guidelines for computing crop water requirements, Food and Agricultural Organization of the United Nations (FAO), 1998.

Arnold, J. G. and Stockle, C. O.: Simulation of supplemental irrigation from on-farm ponds, *Journal of Irrigation and Drainage Engineering*, 117, 408–424, 1991.

Betts, R. A., Boucher, O., Collins, M., Cox, P. M., Falloon, P. D., Gedney, N., Hemming, D. L., Huntingford, C., Jones, C. D., Sexton, D. M. H., and Webb, M. J.: Projected increase in continental runoff due to plant responses to increasing carbon dioxide, *Nature*, 448, 1037–1035, 2007.

Bouwer, L. M., Aerts, J. C. J. H., Droogers, P., and Dolman, A. J.: Detecting the long-term impacts from climate variability and increasing consumption on runoff in the Krishna river basin (India), *Hydrology and Earth Interactions Discussions*, 3, 1249–1280, 2006.

Covich, A. P.: Water and Ecosystems, in: *Water in crisis*, edited by: Gleick, P. H., Oxford University Press, 1993.

Critchley, W., Siebert, K., and Chapman, C.: *Water harvesting. A manual for the design and construction of water harvesting schemes*, FAO, Rome, Italy, 1991.

Dai, A. and Trenberth, K. E.: Estimates of freshwater discharge from continents: latitudinal and seasonal variations, *J. Hydrometeorol.*, 3, 660–687, 2002.

Dai, A., Qian, T., and Trenberth, K. E.: Changes in continental freshwater discharge 1949–2004, *J. Climate*, accepted, 2008.

Dickonson, R. E., Zebiak, S. E., Anderson, J. L., Blackmon, M. L., Luca, C. D., Hogan, T. F., Iredell, M., Ji, M., Rood, R. B., Suarez, M. J., and Taylor, K. E.: How can we advance our weather and climate model as a community?, *B. Am. Meteor. Soc.*, 83, 431–434, 2002.

Dingman, L. S.: Analytical derivation of at-a-station hydraulic geometry relations, *J. Hydrology*, 334, 17–27, 2007.

Döll, P. and Lehner, B.: Validation of a new global 30-min drainage direction map, *J. Hydrology*, 258, 214–231, 2002.

- Döll, P. and Siebert, S.: Global modelling of irrigation water requirements, *Water Resour. Res.*, 38, 82–810, 2002.
- Döll, P., Kaspar, F., and Lehner, B.: A global hydrological model for deriving water availability indicators: model tuning and validation, *J. Hydrology*, 270, 103–134, 2003.
- 5 Douglas, E. M., Niyogi, D., Frohling, S., Yelurpudi, J., Pielke Sr, R., Niyogi, N., Vörösmarty, C. J., and Mohanty, U. C.: Changes in Moisture and energy fluxes due to agricultural land use and irrigation in the Indian Monsoon Belt, *Geophys. Res. Lett.*, 33, L14403, doi:10.1029/2006GL026550, 2006.
- Federer, C. A., Vörösmarty, C. J., and Fekete, B.: Sensitivity of annual evaporation to soil and root properties in two models of contrasting complexity, *J. Hydrometeorol.*, 4, 1276–1290, 10 2003.
- Fekete, B. M., Vörösmarty, C. J., and Grabs, W.: Global, composite runoff fields based on observed river discharge and simulated water balances, Global Runoff Data Centre (GRDC), Report 22, 1999.
- 15 Fekete, B. M., Vörösmarty, C. J., and Grabs, W.: High-resolution fields of global runoff by combining observed river discharge and simulated water balances, *Global Biogeochem. Cy.*, 16(3), 1042, doi:10.1029/1999GB001254, 2002.
- Fekete, B. M., Vörösmarty, C. J., Roads, J. O., and Willmott, C. J.: Uncertainties in precipitation and their impacts on runoff estimates, *J. Climate*, 17, 294–304, 2004.
- 20 Foster, S. S. D. and Chilton, P. J.: Groundwater: the processes and global significance of aquifer degradation, *Philosophical Transactions of the Royal Society B*, 358, 1957–1972, 2003.
- Freydank, K. and Siebert, S.: Towards mapping the extent of irrigation in the last century: time series of irrigated area per country, Institute of Physical Geography, University of Frankfurt, Frankfurt am Main, Germany, Frankfurt Hydrology Paper 08, 2008.
- 25 Galy-Lacaux, C., Delmas, R., Kouadio, G., Richard, S., and Gosse, P.: Long-term greenhouse gas emissions from hydroelectric reservoirs in tropical forest regions, *Global Biogeochem. Cy.*, 13, 503–518, 1999.
- Geng, S., de Fries, F. W. T. P., and Supit, I.: A simple method for generating daily rainfall data, *Agricultural and Forest Meteorology*, 36, 363–376, 1986.
- 30 Ghassemi, F. and White, I.: Inter-basin water transfer: case studies from Australia, United States, Canada, China, and India, *International Hydrology Series*, Cambridge University Press, 2007.
- Gordon, L. J., Steffen, W., Jönsson, B. F., Folke, C., Falkenmark, M., and Johannssen, A. A.:

## Reconstructing 20th century global hydrography

D. Wisser et al.

Title Page

Abstract

Introduction

Conclusions

References

Tables

Figures

◀

▶

◀

▶

Back

Close

Full Screen / Esc

Printer-friendly Version

Interactive Discussion



Human modifications of global water vapor flows from the land surface, Proceedings of the National Academy of Science, 102, 7612–7617, 2005.

Haddeland, I., Lettenmaier, D. P., and Skaugen, T.: Effects of irrigation on the water and energy balances of the Colorado and Mekong river basins, J. Hydrology, 324, 210–223, 2006a.

5 Haddeland, I., Skaugen, T., and Lettenmaier, D. P.: Anthropogenic impacts on continental surface water fluxes, Geophys. Res. Lett., 33, L08406, doi:10.1029/2006GL026047, 2006b.

Haddeland, I., Skaugen, T., and Lettenmaier, D. P.: Hydrologic effects of land and water management in North America and Asia: 17001992, Hydrol. Earth Syst. Sci., 11, 1035–1045, 2007,

10 <http://www.hydrol-earth-syst-sci.net/11/1035/2007/>.

Hamon, W. R.: Computation of direct runoff amounts from storm rainfall, Int. Assoc. Sci. Hydrol. Publ., 63, 52–62, 1963.

Hanasaki, N., Kanae, S., and Oki, T.: A reservoir operation scheme for global river routing models, J. Hydrology, 327, 22–41, 2006.

15 Hanasaki, N., Kanae, S., Oki, T., Masuda, K., Motoya, K., Shirakawa, N., Shen, Y., and Tanaka, K.: An integrated model for the assessment of global water resources - Part 2: Applications and assessments, Hydrol. Earth Syst. Sci., 12, 1027–1037, 2008, <http://www.hydrol-earth-syst-sci.net/12/1027/2008/>.

Huffman, G. J., Adler, R. F., Morrissey, M., Bolvin, D. T., Curtis, S., Joyce, R., McGavock, B., and Susskind, J.: Global Precipitation at One-Degree Daily Resolution from Multi-Satellite Observations, J. Hydrometeorol., 2, 36–50, 2001.

20 Hulme, M., Osborn, T. J., and Johns, T. C.: Precipitation sensitivity to global warming: comparison of observations with HadCM2 simulations, Geophys. Res. Lett., 25(17), 3379–3382, 1998.

25 Hunger, M. and Döll, P.: Value of river discharge data for global-scale hydrological modeling, Hydrol. Earth Syst. Sci., 12, 841–861, 2008, <http://www.hydrol-earth-syst-sci.net/12/841/2008/>.

ICOLD: World Register of Dams, International Commission on Large Dams ICOLD, 1998.

ICOLD: World Register of Dams, International Commission on Large Dams ICOLD, 2003.

30 Kendy, E. and Bredehoeft, J. D.: Transient effects of groundwater pumping and surface-water-irrigation returns on streamflow, Water Resour. Res., 42, W08415, doi:10.1029/2005WR004792, 2006.

Knighton, D.: Fluvial Processes, Hodder Arnold, 1998.

# HESSD

6, 2679–2732, 2009

## Reconstructing 20th century global hydrography

D. Wisser et al.

Title Page

Abstract

Introduction

Conclusions

References

Tables

Figures

◀

▶

◀

▶

Back

Close

Full Screen / Esc

Printer-friendly Version

Interactive Discussion



Kueppers, L. M., Snyder, M. A., and Sloan, L. C.: Irrigation cooling effect: regional climate forcing by land-use change, *Geophys. Res. Lett.*, 34, L03703, doi:10.1029/2006GL028679, 2007.

Labat, D., Godderis, Y., Probst, J. L., and Guyot, J. L.: Evidence for global runoff increase related to climate warming, *Adv. Water Res.*, 27, 631–642, 2004.

Lehner, B., Verdin, K., and Jarvis, A.: New global hydrography derived from spaceborne elevation data, *EOS Transactions*, 89, 93–94, 2008.

Lettenmaier, D. P.: Macroscale hydrology: Challenges and opportunities, in: Present and future of modeling global environmental change: toward integrated modeling, edited by: Matsuno, T., and Kida, H., TERRAPUB, 111–136, 2001.

Macleane, J. L., Dawe, D. C., Hardz, B., and Hettel, G. P.: *Rice almanac*, CAB Publishing, 2002.

McCully, P.: *Silenced rivers: the ecology and politics of large dams*, Zed books, London, UK, 1996.

Micklin, P.: The Aral Sea disaster, *Annual Review of Earth and Planetary Sciences*, 35, 47–72, 2007.

Milliman, J. D., Farnsworth, K. L., Jones, P. D., Xu, K. H., and Smith, L. C.: Climatic and anthropogenic factors affecting river discharge to the global ocean, 1951–2000, *Global and Planetary Change*, 62, 187–194, 2008.

Milly, P. C. D., Dunne, K. A., and Vecchia, A. V.: Global pattern of trends in streamflow and water availability in a changing climate, *Nature*, 437, 347–350, 2005.

Mitchell, T. D. and Jones, P. D.: An improved method of constructing a database of monthly climate observations and associated high-resolution grids, *International J. Climatol.*, 25, 693–712, 2005.

Monfreda, C., Ramankutty, N., and Foley, J. A.: Farming the planet: 2. Geographic distribution of crop areas, yields, physiological types, and net primary production in the year 2000, *Global Biogeochem. Cy.*, 22, GB1022, doi:10.1029/2007GB002947, 2008.

Moore, N. and Rojstaczer, S.: Irrigation-induced rainfall and the great plains, *J. Appl. Meteorol.*, 40, 1297–1309, 2001.

Oki, T. and Sud, Y. C.: Design of total runoff integrating pathways (TRIP) – A global river channel network, *Earth Interactions*, 2, 2–36, 1998.

Oki, T. and Kanae, S.: Global hydrological cycles and world water resources, *Science*, 313, 1068–1072, 2006.

Peterson, B. J., Holmes, R. M., McClelland, J. W., Vorosmarty, C. J., Lammers, R. B., Shiklo-

## Reconstructing 20th century global hydrography

D. Wisser et al.

Title Page

Abstract

Introduction

Conclusions

References

Tables

Figures

◀

▶

◀

▶

Back

Close

Full Screen / Esc

Printer-friendly Version

Interactive Discussion



- manov, A. I., Shiklomanov, I. A., and Rahmstorf, S.: Increasing river discharge to the Arctic Ocean, *Science*, 298, 2171–2173, 2002.
- Piao, S., Friedlingstein, P., Ciais, P., Noblet-Ducoudre, N. D., Labat, D., and Zaehle, S.: Changes in climate and land use have a larger direct impact than rising CO<sub>2</sub> on global river runoff trends, *PNAS*, 104, 15242–15247, 2007.
- Pimentel, D., Berger, B., Filiberto, D., Newton, M., Wolfe, B., Karabinakis, E., Clark, S., Poon, E., Abbet, E., and Nandagopal, S.: Water resources: Agricultural and environmental issues, *BioScience*, 54, 909–918, 2004.
- Ponce, V. M.: *Engineering Hydrology: Principles and Practices*, Prentice Hall, 1994.
- Qian, T., Dai, A., and Trenberth, K. E.: Hydroclimatic trends in the Mississippi river basin from 1948 to 2004, *J. Climate*, 20, 4599–4613, 2007.
- Rawlins, M. A., Lammers, R. B., Frohling, S., Fekete, B. M., and Vorosmarty, C. J.: Simulating pan-Arctic runoff with a macro-scale terrestrial water balance model, *Hydrol. Process.*, 17, 2521–2539, 2003.
- Rawlins, M. A., Willmott, C. J., Shiklomanov, A., Linder, E., Frohling, S., Lammers, R. B., and Vorosmarty, C. J.: Evaluation of trends in derived snowfall and rainfall across Eurasia and linkages with discharge to the Arctic Ocean, *Geophys. Res. Lett.*, 33, L07403, doi:10.1029/2005GL025231, 2006.
- Seitzinger, S. P., Styles, R. V., Boyer, E. W., Alexander, R. B., Billen, G., Howarth, R., Mayer, B., and van Breemen, N.: Nitrogen retention in rivers: model development and application to watersheds in the northeastern USA, *Biogeochemistry*, 57, 199–237, 2002.
- Serreze, M. C., Barrett, A. P., Slater, A. G., Woodgate, R. A., Aagaard, K., Lammers, R. B., Steele, M., Moritz, R., Meredith, M., and Lee, C. M.: The large-scale freshwater cycle of the Arctic, *J. Geophys. Res.-Oceans*, 111, C11010, doi:10.1029/2005JC003424, 2006.
- Shibuo, Y., Jarsjö, J., and Destouni, G.: Hydrological responses to climate change and irrigation in the Aral Sea drainage basin, *Geophys. Res. Lett.*, 34, L21406, doi:10.1029/2007GL031465, 2007.
- Shiklomanov, I. A. and Rodda, J. C.: *World water resources at the beginning of the 21st century*, {UNESCO} International Hydrology Press ed., Cambridge University Press, 2003.
- Siebert, S., Döll, P., Feick, S., and Hoogeveen, J.: Global map of irrigated areas version 2.2, Johann Wolfgang Goethe University, Frankfurt am Main, Germany / Food and Agriculture Organization of the United Nations, Rome, Italy, 2005a.
- Siebert, S., Döll, P., Hoogeveen, J., Faures, J. M., Frenken, K., and Feick, S.: Development and

---

**Reconstructing 20th century global hydrography**D. Wisser et al.

---

[Title Page](#)[Abstract](#)[Introduction](#)[Conclusions](#)[References](#)[Tables](#)[Figures](#)[◀](#)[▶](#)[◀](#)[▶](#)[Back](#)[Close](#)[Full Screen / Esc](#)[Printer-friendly Version](#)[Interactive Discussion](#)

validation of the global map of irrigated areas, *Hydrology and Earth Systems Sciences*, 9, 535–547, 2005b.

Siebert, S. and Döll, P.: Irrigation water use -a global perspective, in: *Global Change: enough water for all?*, Universität Hamburg/GEO, 104–107, 2007.

5 Singh, D. K. and Singh, A. K.: Groundwater situation in India: Problems and Perspective, *Water Resources Development*, 18, 562–580, 2002.

Sitch, S., Smith, B., Prentice, I. C., Arneth, A., Bondeau, A., Cramer, W., Kaplan, J. O., Levis, S., Lucht, W., Sykes, M. T., Thonicke, K., and Venevsky, S.: Evaluation of ecosystem dynamics, plant geography and terrestrial carbon cycling in the LPJ dynamic global vegetation model, *Global Change Biology*, 9, 161–185, 2003.

10 Snoussi, M., Hiada, S., and Imassi, S.: Effects of the construction of dams on the water and sediment fluxes of the Moulouya and the Sebou rivers, Morocco, *Regional Environmental Change*, 3, 5–12, 2002.

Soumis, N., Duchemin, E., Canuel, R., and Lucotte, M.: Greenhouse gas emissions from reservoir in the western United States, *Global Biogeochem. Cy.*, 18, GB3022, doi:10.109/2003GB002197, 2004.

Srivastava, R. C.: Design of runoff recycling irrigation system for rice cultivation, *Journal of Irrigation and Drainage Engineering*, 122, 331–335, 1996.

20 Srivastava, R. C.: Methodology for design of water harvesting system for high rainfall areas, *Agr. Water Manag.*, 47, 37–53, 2001.

St. Louis, V., Kelly, C. A., Duchemin, E., Rudd, J. W. M., and Rosenberg, D. M.: Reservoir surfaces as sources of greenhouse gases to the atmosphere: A global estimate, *BioScience*, 50, 766–775, 2000.

25 Thenkabail, P. S., Biradar, C. M., Turrall, H., Noojipady, P., Li, Y. J., Vithanage, J., Dheeravath, V., Velpuri, M., M, S., Cai, X. L., and Dutta, R.: An Irrigated Area Map of the World (1999) derived from Remote Sensing, International Water Management Institute (IWMI), 2006.

Tian, X., Dai, A., Yang, D., and Xie, Z.: Effects of precipitation-bias correction on surface hydrology over northern latitudes, *Geophysical Research Letters*, 112, D14101, doi:10.1029/2007JD008420, 2007.

30 Trenberth, K. E. and Dai, A.: Effects of Mount Pinatubo volcanic eruption on the hydrological cycle as an analog of geoengineering, *Geophys. Res. Lett.*, 34, L15702, doi:10.1029/2007GL030524, 2007.

Vörösmarty, C. J., Willmott, C. H., Choudhury, B. J., Schloss, A. L., Strains, T. K., Robeson,

## Reconstructing 20th century global hydrography

D. Wisser et al.

Title Page

Abstract

Introduction

Conclusions

References

Tables

Figures

◀

▶

◀

▶

Back

Close

Full Screen / Esc

Printer-friendly Version

Interactive Discussion



## Reconstructing 20th century global hydrography

D. Wisser et al.

Title Page

Abstract

Introduction

Conclusions

References

Tables

Figures

◀

▶

◀

▶

Back

Close

Full Screen / Esc

Printer-friendly Version

Interactive Discussion



S. M., and Dorman, T. J.: Analyzing the discharge regime of a large tropical river through remote sensing, ground-based climatic data and modeling, *Water Resour. Res.*, 32, 3137–3150, 1996.

Vörösmarty, C. J., Sharma, K. P., Fekete, B. M., Copeland, A. H., Holden, J., Marble, J., and Lough, J. A.: The storage and aging of continental runoff in large reservoir systems of the world, *Ambio*, 26, 210–219, 1997.

Vörösmarty, C. J., Federer, C. A., and Schloss, A. L.: Potential Evaporation functions compared on US watersheds: Implications for global-scale water balance and terrestrial ecosystem modeling, *J. Hydrology*, 207, 147–169, 1998.

Vörösmarty, C. J., Fekete, B. M., Meybeck, M., and Lammers, R. B.: A simulated topological network representing the global system of rivers at 30-minute spatial resolution (STN-30), *Global Biogeochem. Cy.*, 14, 599–621, 2000a.

Vörösmarty, C. J., Fekete, B. M., Meybeck, M., and Lammers, R. B.: Geomorphometric attributes of the global system of rivers at 30-minute spatial resolution (STN-30), *J. Hydrology*, 237, 17–39, 2000b.

Vörösmarty, C. J., Green, P., Salisbury, J., and Lammers, R. B.: Global Water Resources: Vulnerability from Climate Change and Population Growth, *Science*, 289(5477), 284–288, 2000c.

Vörösmarty, C. J. and Sahagian, D.: Anthropogenic disturbance of the terrestrial water cycle, *BioScience*, 50, 753–765, 2000.

Vörösmarty, C. J.: Global Water Assessment and potential contributions form Earth Systems Science, *Aquat. Sci.*, 64, 328–351, 2002.

Vörösmarty, C. J., Meybeck, M., Fekete, B. M., Sharma, K., Green, P., and Syvitski, J.: Anthropogenic sediment retention: Major global-scale impact from the population of registered impoundments, *Global and Planetary Change*, 39, 169–190, 2003.

Vörösmarty, C. J., C. Leveque, C. Revenga (Convening Lead Authors), Caudill, C., Chilton, J., Douglas, E. M. (Coordinating Lead Authors): Michel Meybeck, Daniel Prager. Chapter 7: Fresh Water Ecosystems, In: Millenium Ecosystem Assessment, Volume 1: Condition and Trends Working Group Report, Island Press, 2005.

Vörösmarty, C. J., Ericson, J. P., Dingman, S. L., Ward, L. G., and Meybeck, M.: Future impacts of fresh water resource management: sensitivity of coastal deltas, *Water Quality and Sediment Behaviour of the Future: Predictions for the 21st Century*, Perugia, Italy, 2007.

Willmott, C. J.: On the validation of models, *Physical Geography*, 1, 184–194, 1981.

Willmott, C. J., Rowe, C. N., and Mintze, Y.: Climatology of the terrestrial seasonal water cycle, *J. Climatol.*, 43, 495–511, 1985.

Wisser, D., Frolking, S., Douglas, E. M., Fekete, B. M., and Vörösmarty, C. J.: Global irrigation water demand: Variability and uncertainties arising from agricultural and climate data sets, *Geophys. Res. Lett.*, 35, L24408, doi:10.1029/2008GL035296, 2008.

Wollheim, W. M., Vörösmarty, C. J., Bouwman, A. F., Green, P., Harrison, J., Linder, E., Peterson, B. J., Seitzinger, S. P., and Syvitski, J. P. M.: Global N removal by freshwater aquatic systems using a spatially distributed, within basin approach, *Global Biogeochem. Cy.*, 22, GB2026, doi:10.1029/2007GB002963, 2008.

**HESSD**

6, 2679–2732, 2009

---

## Reconstructing 20th century global hydrography

D. Wisser et al.

---

Title Page

Abstract

Introduction

Conclusions

References

Tables

Figures

◀

▶

◀

▶

Back

Close

Full Screen / Esc

Printer-friendly Version

Interactive Discussion



Reconstructing 20th century global hydrography

D. Wisser et al.

**Table 1.** Modeld water withdrawl from different sources under contemporay conditions.

| Water source          | Water withdrawal [km <sup>3</sup> a <sup>-1</sup> ] | Percentage of total withdrawal |
|-----------------------|---|--------------------------------|
| Small Reservoirs      | 989   | 33                             |
| Local groundwater     | 509   | 17                             |
| River discharge       | 300   | 10                             |
| Non-renewable sources | 1199  | 40                             |
| Global total          | 2997  | 100                            |

Title Page

Abstract

Introduction

Conclusions

References

Tables

Figures



Back

Close

Full Screen / Esc

Printer-friendly Version

Interactive Discussion



**Table 2.** Components of the hydrological cycle for endorheic basins and basins draining into the Oceans. Fluxes in  $\text{km}^3 \text{a}^{-1}$ . Coefficient of variation (CV) calculated from monthly flows. nat.: model run under natural conditions, dist: model results under disturbed conditions (irrigation water abstractions and reservoir operation turned on)  $P$ =precipitation,  $ET$ =evapotranspiration,  $Q$ =discharge.

| Ocean                   | 1901/1925 |         | 1926/1950 |         | 1951–1975 |         | 1976–2002 |         | 1901–2002 |         | Fekete 2002 |
|-------------------------|-----------|---------|-----------|---------|-----------|---------|-----------|---------|-----------|---------|-------------|
|                         | nat.      | dist.   |             |
| Land                    | $P$       | 5799    |           | 5728    |           | 5949    |           | 5917    |           | 5849    |             |
|                         | $ET$      | 4718    | 4764      | 4652    | 4713      | 4793    | 4893      | 4863    | 5012      | 4752    | 4849        |
|                         | $Q$       | 1060    | 1040      | 1062    | 1033      | 1137    | 1097      | 1032    | 984       | 1072    | 1037        |
|                         | CV        | 0.51    | 0.51      | 0.5     | 0.49      | 0.51    | 0.42      | 0.52    | 0.37      | 0.51    | 0.45        |
| Mediterranean/Black Sea | $P$       | 4922    |           | 4912    |           | 5003    |           | 4777    |           | 4901    |             |
|                         | $ET$      | 3887    | 3720      | 3688    | 3728      | 3707    | 3765      | 3657    | 3752      | 3684    | 3742        |
|                         | $Q$       | 1205    | 1188      | 1213    | 1191      | 1280    | 1236      | 1098    | 1066      | 1197    | 1168        |
|                         | CV        | 0.28    | 0.28      | 0.29    | 0.29      | 0.27    | 0.27      | 0.29    | 0.34      | 0.29    | 0.30        |
| Arctic                  | $P$       | 7613    |           | 7809    |           | 8083    |           | 8018    |           | 7884    |             |
|                         | $ET$      | 4445    | 4446      | 4615    | 4616      | 4561    | 4562      | 4612    | 4614      | 4559    | 4561        |
|                         | $Q$       | 2101    | 2101      | 2185    | 2185      | 2480    | 2462      | 2379    | 2375      | 2288    | 2282        |
|                         | CV        | 1.03    | 1.03      | 0.96    | 0.96      | 1.01    | 0.97      | 1.00    | 0.93      | 1.00    | 0.97        |
| Pacific                 | $P$       | 21 641  |           | 21 857  |           | 22 394  |           | 21 827  |           | 21 928  |             |
|                         | $ET$      | 11 979  | 12 166    | 12 086  | 12 327    | 12 020  | 12 388    | 12 182  | 12 734    | 12 069  | 12 410      |
|                         | $Q$       | 9666    | 9518      | 9746    | 9564      | 10 357  | 10 095    | 9658    | 9350      | 9853    | 9626        |
|                         | CV        | 0.19    | 0.19      | 0.19    | 0.19      | 0.20    | 0.18      | 0.19    | 0.17      | 0.20    | 0.18        |
| Atlantic                | $P$       | 50 215  |           | 50 166  |           | 51 072  |           | 50 931  |           | 50 602  |             |
|                         | $ET$      | 32 129  | 32 153    | 32 117  | 32 150    | 32 275  | 32 330    | 32 660  | 32 742    | 32 302  | 32 352      |
|                         | $Q$       | 18 106  | 18 088    | 18 084  | 18 060    | 18 825  | 18 778    | 18 344  | 18 296    | 18 340  | 18 305      |
|                         | CV        | 0.23    | 0.23      | 0.24    | 0.23      | 0.23    | 0.22      | 0.26    | 0.24      | 0.24    | 0.23        |
| Indian                  | $P$       | 15 109  |           | 15 204  |           | 15 579  |           | 15 294  |           | 15 296  |             |
|                         | $ET$      | 9925    | 10 025    | 9869    | 10 292    | 10 048  | 10 612    | 10 193  | 11 063    | 10 012  | 10 566      |
|                         | $Q$       | 5133    | 4953      | 5274    | 5059      | 5477    | 5196      | 5065    | 4742      | 5234    | 4983        |
|                         | CV        | 0.33    | 0.30      | 0.34    | 0.31      | 0.33    | 0.29      | 0.33    | 0.30      | 0.33    | 0.30        |
| Global                  | $P$       | 105 298 |           | 106 675 |           | 108 081 |           | 106 764 |           | 106 461 |             |
|                         | $ET$      | 67 083  | 68 274    | 67 027  | 67 826    | 67 404  | 68 550    | 68 167  | 69 917    | 67 378  | 68 480      |
|                         | $Q$       | 37 271  | 36 888    | 37 564  | 37 092    | 39 556  | 38 864    | 37 576  | 36 813    | 37 984  | 37 401      |
|                         | CV        | 0.19    | 0.19      | 0.2     | 0.19      | 0.19    | 0.18      | 0.21    | 0.18      | 0.20    | 0.19        |

Title Page

Abstract Introduction

Conclusions References

Tables Figures

◀ ▶

◀ ▶

Back Close

Full Screen / Esc

Printer-friendly Version

Interactive Discussion



## Reconstructing 20th century global hydrography

D. Wisser et al.

**Table 3.** Characteristics of endorheic basins and basins draining into the Oceans and computed trends in modeled annual discharge 1901–2002 (significant trends in bold). Irrigated areas and reservoir capacities based on 2002 data. Residence time is computed as total reservoir volume over mean annual runoff; taken from Fekete et al. (2002). Basin delineation based on the STN-30 river network.

| Ocean                   | Area [km <sup>2</sup> ] | Reservoir Capacity [km <sup>3</sup> ] | Irrigated Area [km <sup>2</sup> ] | Irrigated Area [%] | Residence Time [a] | Trend (natural) | Trend (disturbed) |
|-------------------------|-------------------------|---------------------------------------|-----------------------------------|--------------------|--------------------|-----------------|-------------------|
| Land                    | 18 743 062              | 290                                   | 271 121                           | 1.45               | 0.29               | −0.21           | −0.54             |
| Mediterranean/Black Sea | 10 678 622              | 506                                   | 233 241                           | 2.18               | 0.42               | <b>−1.19</b>    | −1.41             |
| Atlantic Ocean          | 45 729 720              | 1904                                  | 362 296                           | 0.79               | 0.10               | 5.84            | 5.41              |
| Indian Ocean            | 20 688 590              | 611                                   | 927 762                           | 4.48               | 0.13               | −0.14           | −2.07             |
| Pacific Ocean           | 19 931 492              | 742                                   | 826 268                           | 4.15               | 0.07               | 2.71            | 0.51              |
| Arctic Ocean            | 19 824 778              | 673                                   | 12 472                            | 0.06               | 0.21               | <b>4.25</b>     | <b>4.13</b>       |
| Global                  | 135 596 264             | 4726                                  | 2 633 160                         | 1.94               | 0.12               | 11.27           | 6.02              |

Title Page

Abstract

Introduction

Conclusions

References

Tables

Figures

◀

▶

◀

▶

Back

Close

Full Screen / Esc

Printer-friendly Version

Interactive Discussion



## Reconstructing 20th century global hydrography

D. Wisser et al.

**Table 4.** River storage volume and apparent age of water entering the Oceans and endorheci basins.

| Ocean         | $V_{\text{riv}}$ [km <sup>3</sup> ] | $\tau_m$ (natural) [d] | $\tau_m$ (2002) [d] | $\Delta\tau_m$ [d] |
|---------------|-------------------------------------|------------------------|---------------------|--------------------|
| Pacific       | 192                                 | 8                      | 38                  | 30                 |
| Atlantic      | 1143                                | 24                     | 56                  | 32                 |
| Indian        | 142                                 | 12                     | 57                  | 45                 |
| Land          | 50                                  | 20                     | 143                 | 123                |
| Mediterranean | 105                                 | 39                     | 205                 | 166                |
| Arctic        | 133                                 | 24                     | 112                 | 88                 |
| Total         | 1765                                | 19                     | 61                  | 42                 |

Title Page

Abstract

Introduction

Conclusions

References

Tables

Figures

◀

▶

◀

▶

Back

Close

Full Screen / Esc

Printer-friendly Version

Interactive Discussion



Reconstructing 20th century global hydrography

D. Wisser et al.

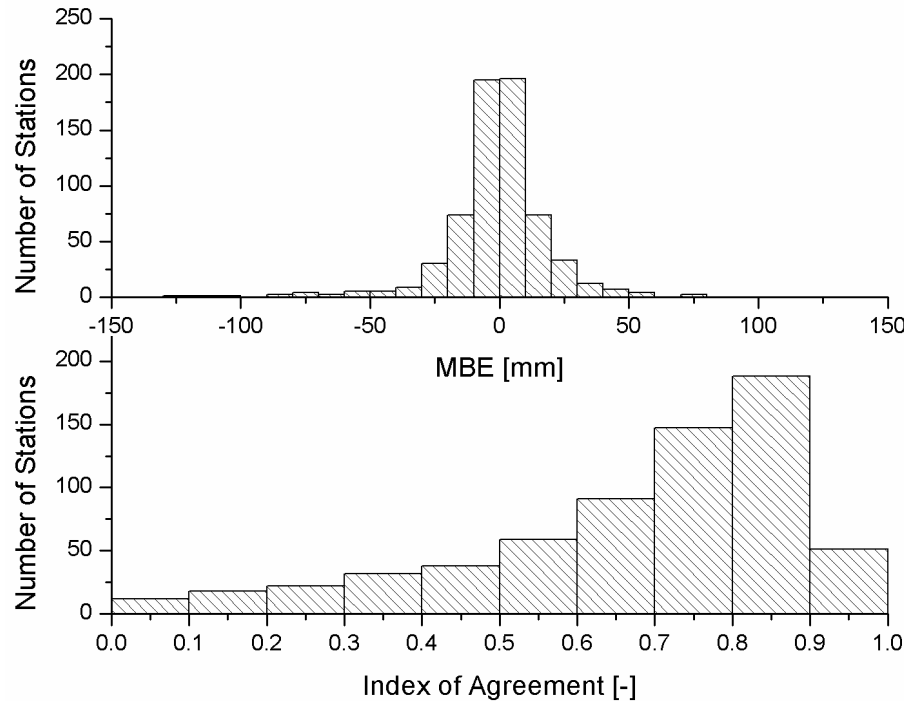


**Fig. 1.** Frequency distribution of the mean model bias for the selected 660 gauging stations. Average MBE is  $-1.2 \text{ mm month}^{-1}$ , average Index of Agreement,  $d$ , 0.68.

Title Page

Abstract

Introduction

Conclusions

References

Tables

Figures

◀

▶

◀

▶

Back

Close

Full Screen / Esc

Printer-friendly Version

Interactive Discussion



Reconstructing 20th century global hydrography

D. Wisser et al.

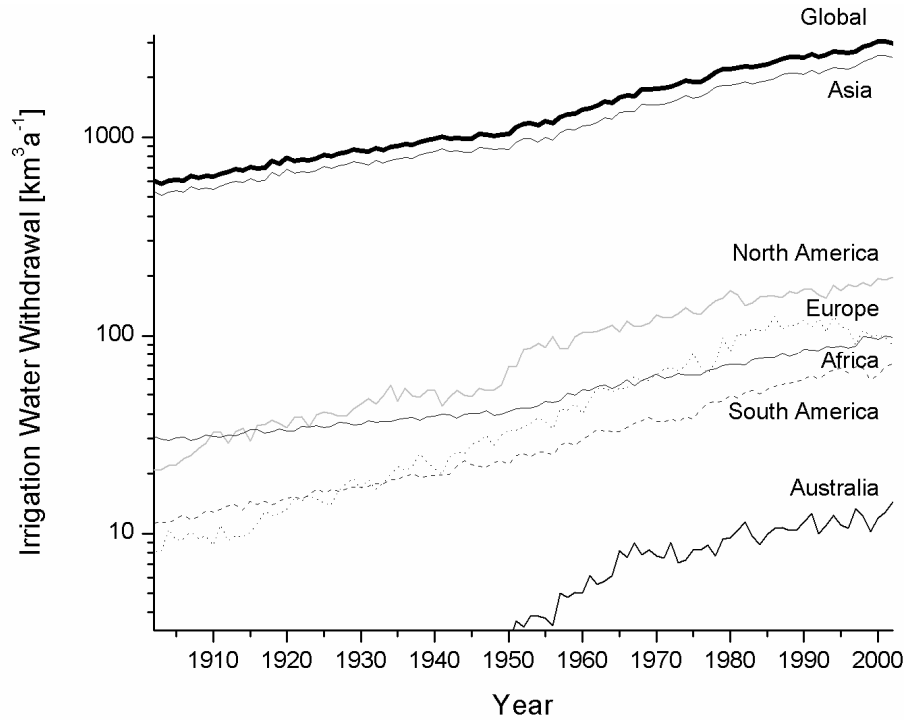


Fig. 2. Time series of modeled irrigation water withdrawal over the last century aggregated by continents.

Title Page

Abstract

Introduction

Conclusions

References

Tables

Figures

◀

▶

◀

▶

Back

Close

Full Screen / Esc

Printer-friendly Version

Interactive Discussion



## Reconstructing 20th century global hydrography

D. Wisser et al.

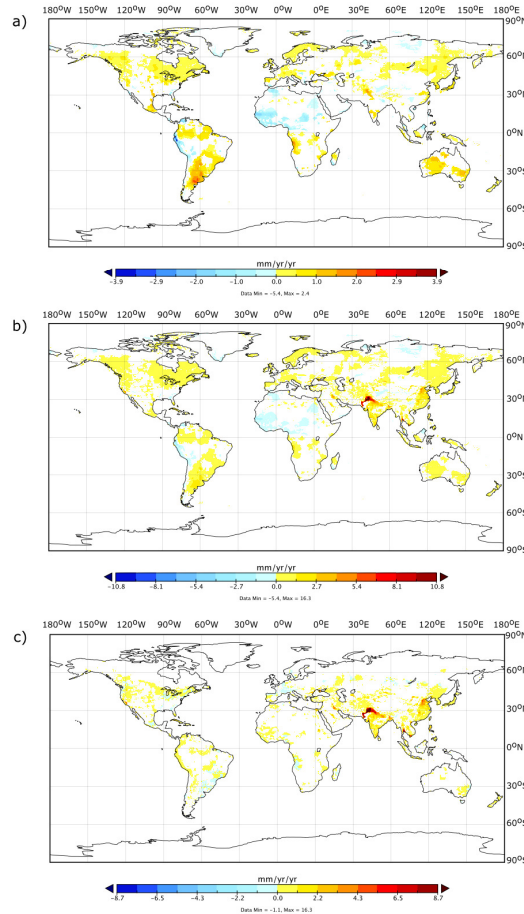


**Fig. 3.** Significant trends [ $\text{mm yr}^{-2}$ ] in modeled annual values of runoff for **(a)** natural, **(b)** disturbed conditions and differences in significant trends between disturbed and natural conditions **(c)** for the period 1901–2002. Trends were tested for significance at the 5% level.

Title Page

Abstract

Introduction

Conclusions

References

Tables

Figures

◀

▶

◀

▶

Back

Close

Full Screen / Esc

Printer-friendly Version

Interactive Discussion



## Reconstructing 20th century global hydrography

D. Wisser et al.

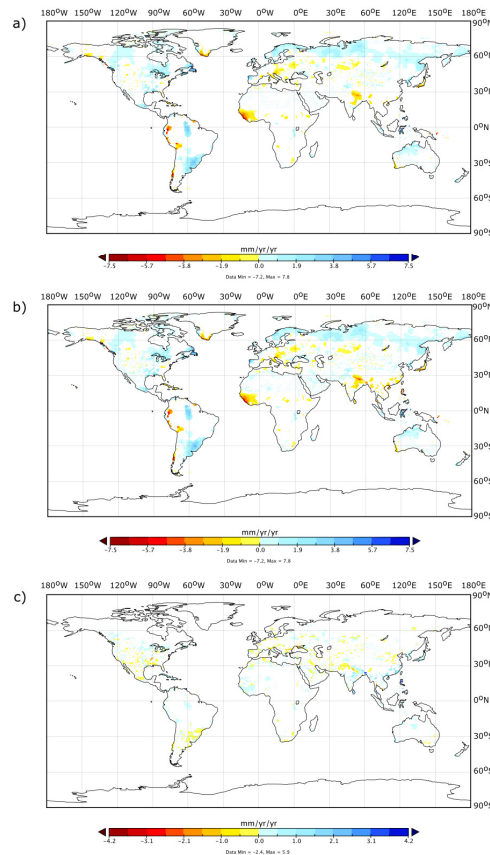


**Fig. 4.** Significant trends [ $\text{mm yr}^{-2}$ ] in modeled annual values of runoff for **(a)** natural, **(b)** disturbed conditions and differences in significant trends between natural and disturbed conditions **(c)** for the period 1901–2002. Small increases in runoff in dry regions under disturbed conditions are caused by return flows from irrigated areas. Trends were tested for significance at the 5% level.

Title Page

Abstract

Introduction

Conclusions

References

Tables

Figures

◀

▶

◀

▶

Back

Close

Full Screen / Esc

Printer-friendly Version

Interactive Discussion



Reconstructing 20th century global hydrography

D. Wisser et al.



Fig. 5. Overview of river basins and receiving oceans, based on the STN-30 river network.

Title Page

Abstract

Introduction

Conclusions

References

Tables

Figures

◀

▶

◀

▶

Back

Close

Full Screen / Esc

Printer-friendly Version

Interactive Discussion



## Reconstructing 20th century global hydrography

D. Wisser et al.

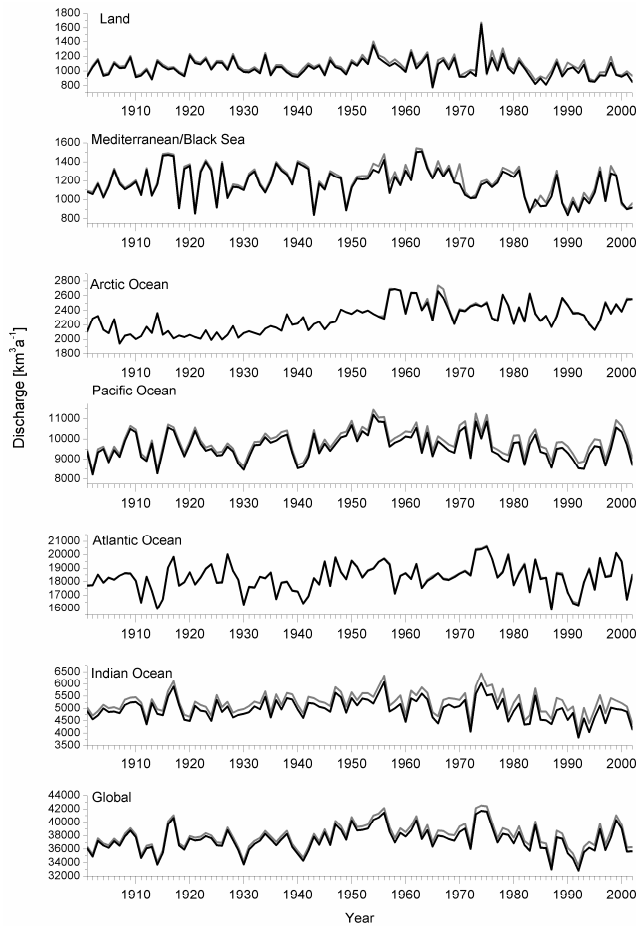


**Fig. 6.** Annual time series of modeled discharge to the ocean and to endorheic basins under natural (gray line) and disturbed (black line) conditions 1901–2002.

Title Page

Abstract

Introduction

Conclusions

References

Tables

Figures

◀

▶

◀

▶

Back

Close

Full Screen / Esc

Printer-friendly Version

Interactive Discussion



## Reconstructing 20th century global hydrography

D. Wisser et al.

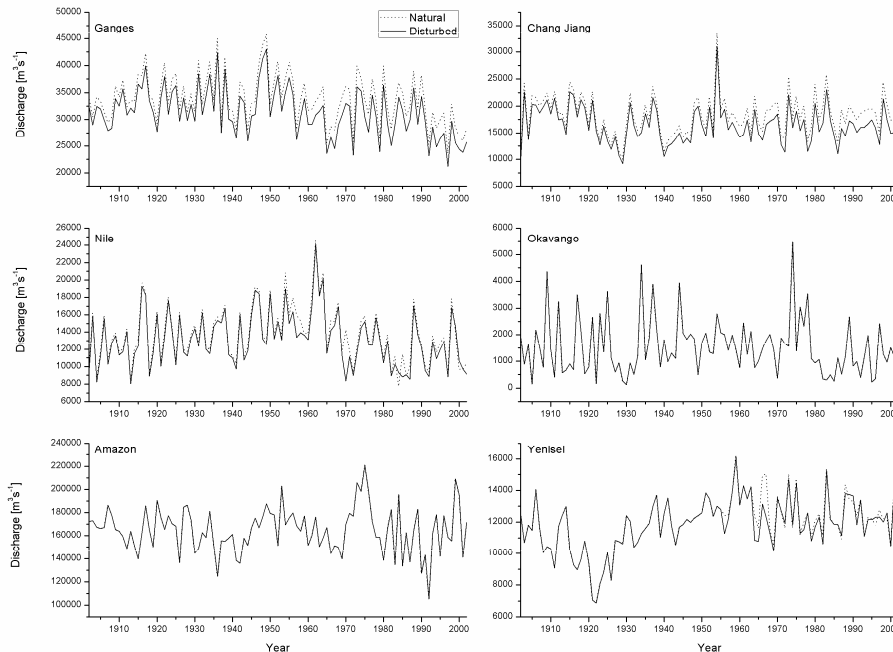


**Fig. 7.** Annual time series of modeled river discharge (at river mouth) under natural and disturbed conditions (1901–2002) for major rivers in different ocean basins: Ganges (Indian Ocean), Nile (Mediterranean), Amazon (Atlantic Ocean), Chang Jiang (Pacific Ocean), Okavango (Internal basin), and Yenisei (Arctic Ocean).

Title Page

Abstract

Introduction

Conclusions

References

Tables

Figures

◀

▶

◀

▶

Back

Close

Full Screen / Esc

Printer-friendly Version

Interactive Discussion



## Reconstructing 20th century global hydrography

D. Wisser et al.

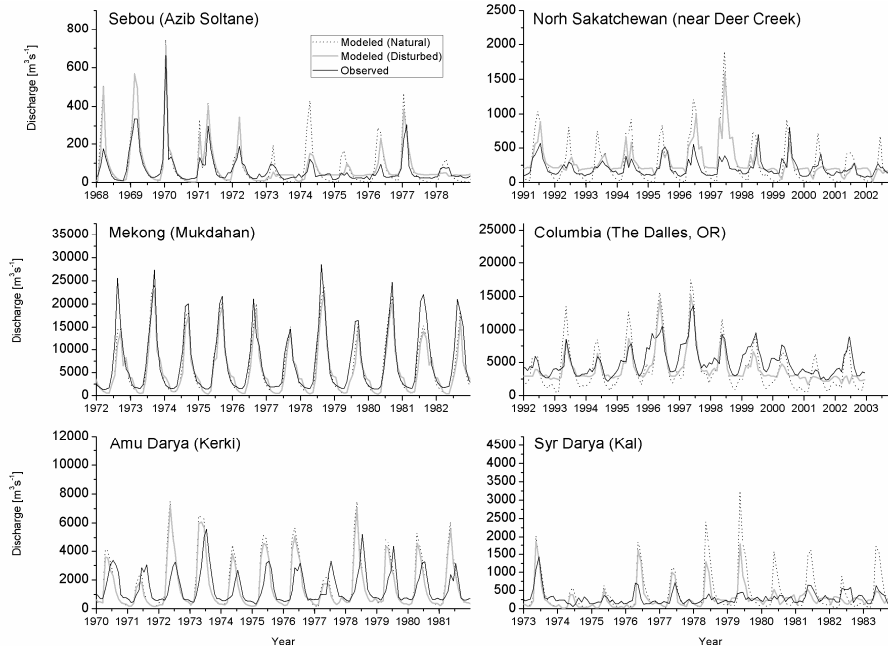


**Fig. 8.** Observed and simulated river discharge (under natural and disturbed) conditions for selected gauging stations.

Title Page

Abstract

Introduction

Conclusions

References

Tables

Figures

◀

▶

◀

▶

Back

Close

Full Screen / Esc

Printer-friendly Version

Interactive Discussion



Reconstructing 20th century global hydrography

D. Wisser et al.

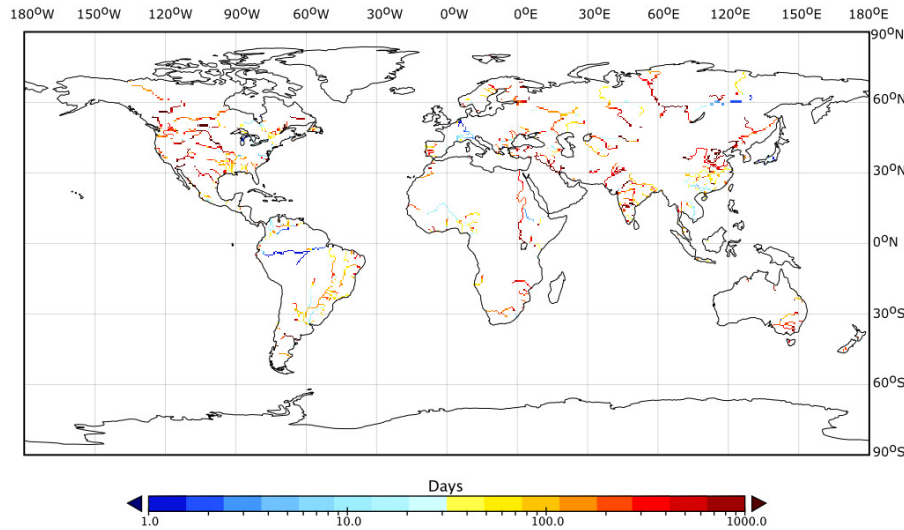


**Fig. 9.** Differences in the apparent aging of water in major rivers under natural and disturbed conditions for the contemporary population of reservoirs.

Title Page

Abstract Introduction

Conclusions References

Tables Figures

◀ ▶

◀ ▶

Back Close

Full Screen / Esc

Printer-friendly Version

Interactive Discussion



Reconstructing 20th century global hydrography

D. Wisser et al.

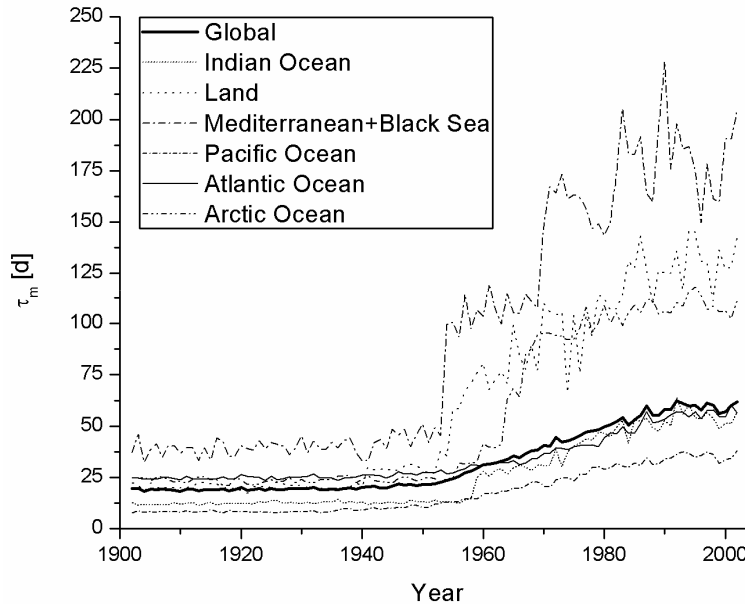


**Fig. 10.** Time series of the discharge weighted apparent water age for discharge entering the oceans and endorheic basins.

Title Page

Abstract

Introduction

Conclusions

References

Tables

Figures

◀

▶

◀

▶

Back

Close

Full Screen / Esc

Printer-friendly Version

Interactive Discussion

